Magnetic Phase Transitions in Zigzag Graphene Nanoribbons at Finite Chemical Potential

Mean-Field Theory and Hybrid Monte Carlo

Lattice 2026 - 28.07.2026

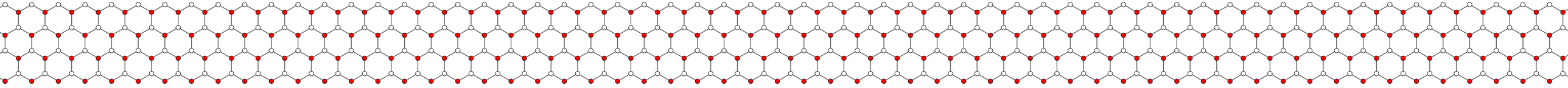

Felix Strohkirch

⟨NuMeriQS⟩

JÜLICH
Forschungszentrum

Motivation

- Experimental evidence for magnetic order phase transitions between narrow and wide zigzag nanoribbons [Magda et al., Nature, 2014]
- Quantum Monte Carlo and mean-field calculations qualitatively agree at moderate Coulomb interactions [Golor et al., Phys. Rev. B, 2013]

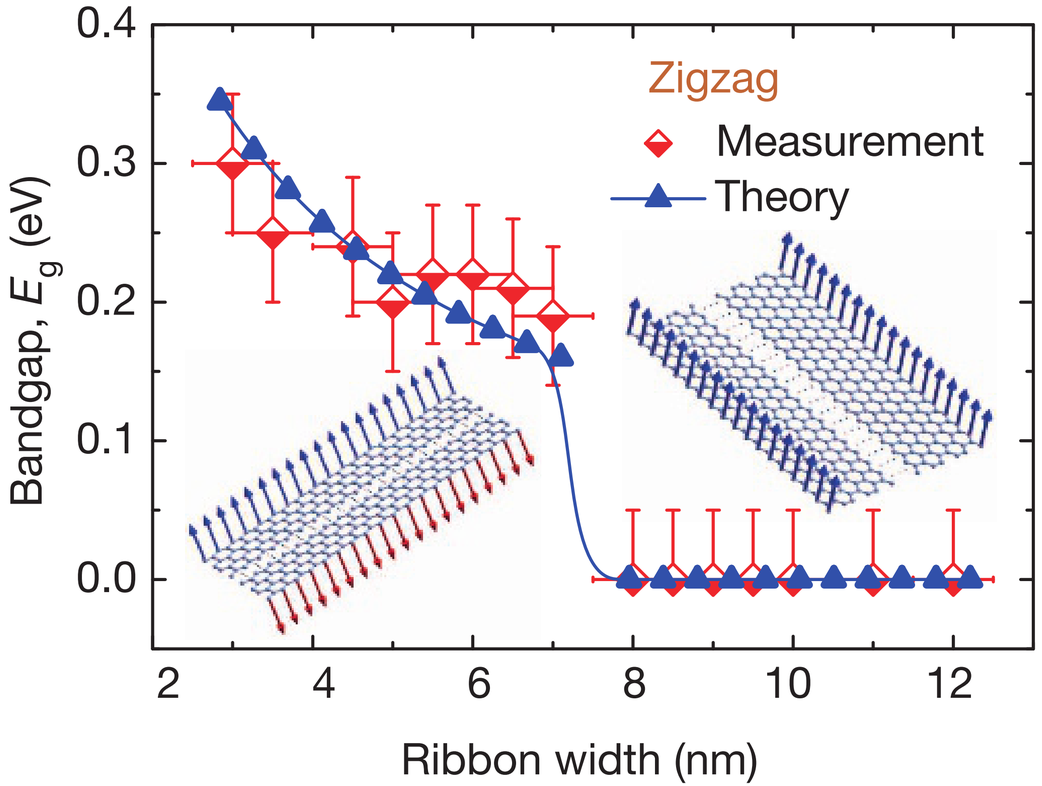

Adapted from Magda et al., Nature, 2014.

Zigzag carbon nanoribbon

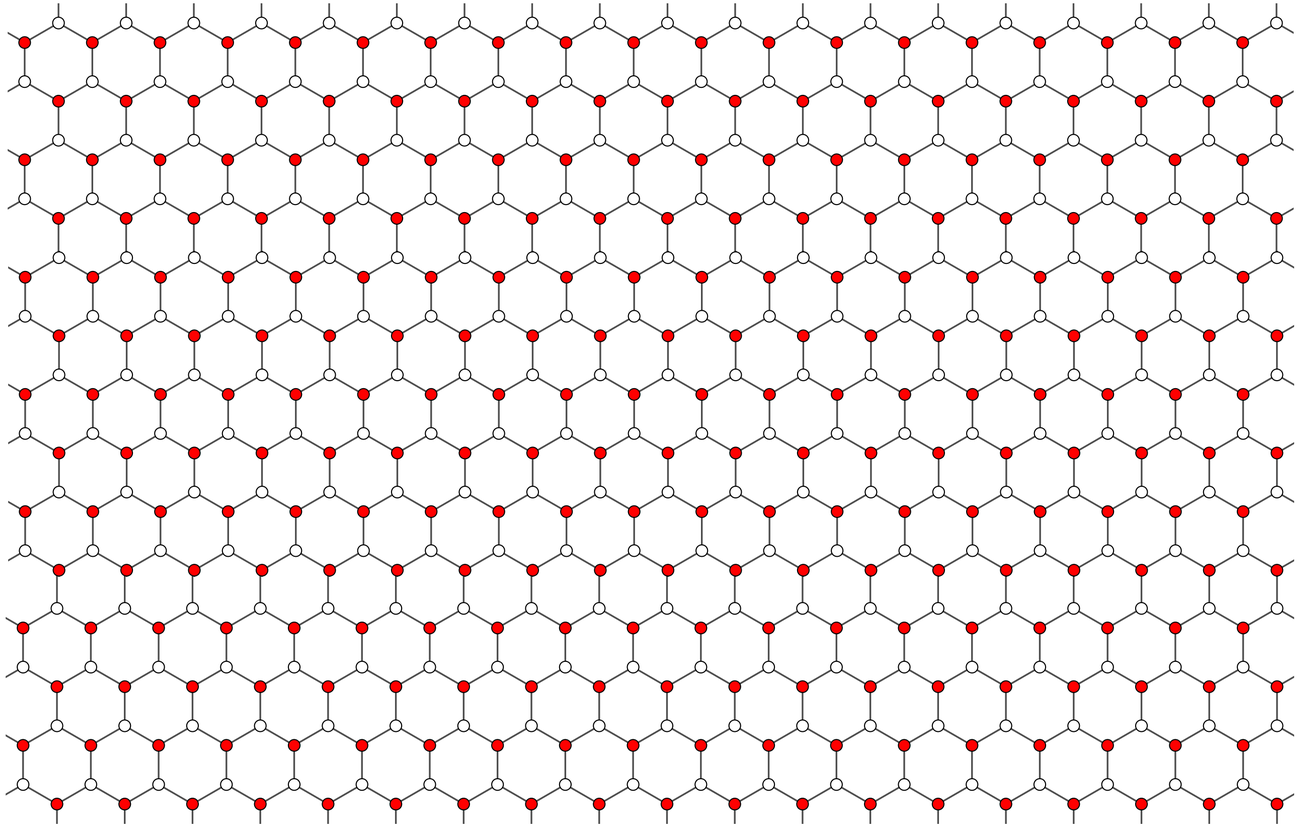

Zigzag carbon nanoribbon

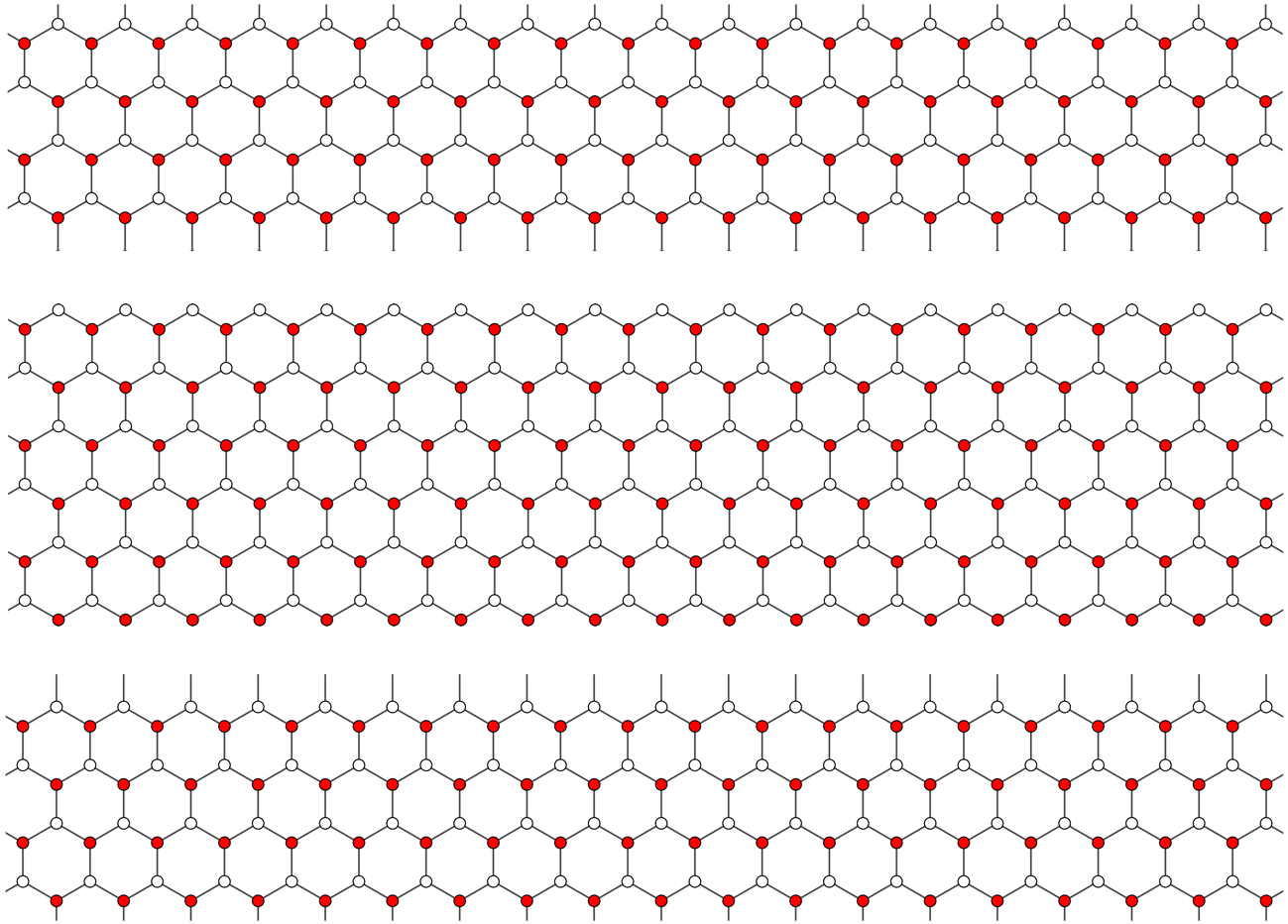

Zigzag carbon nanoribbon

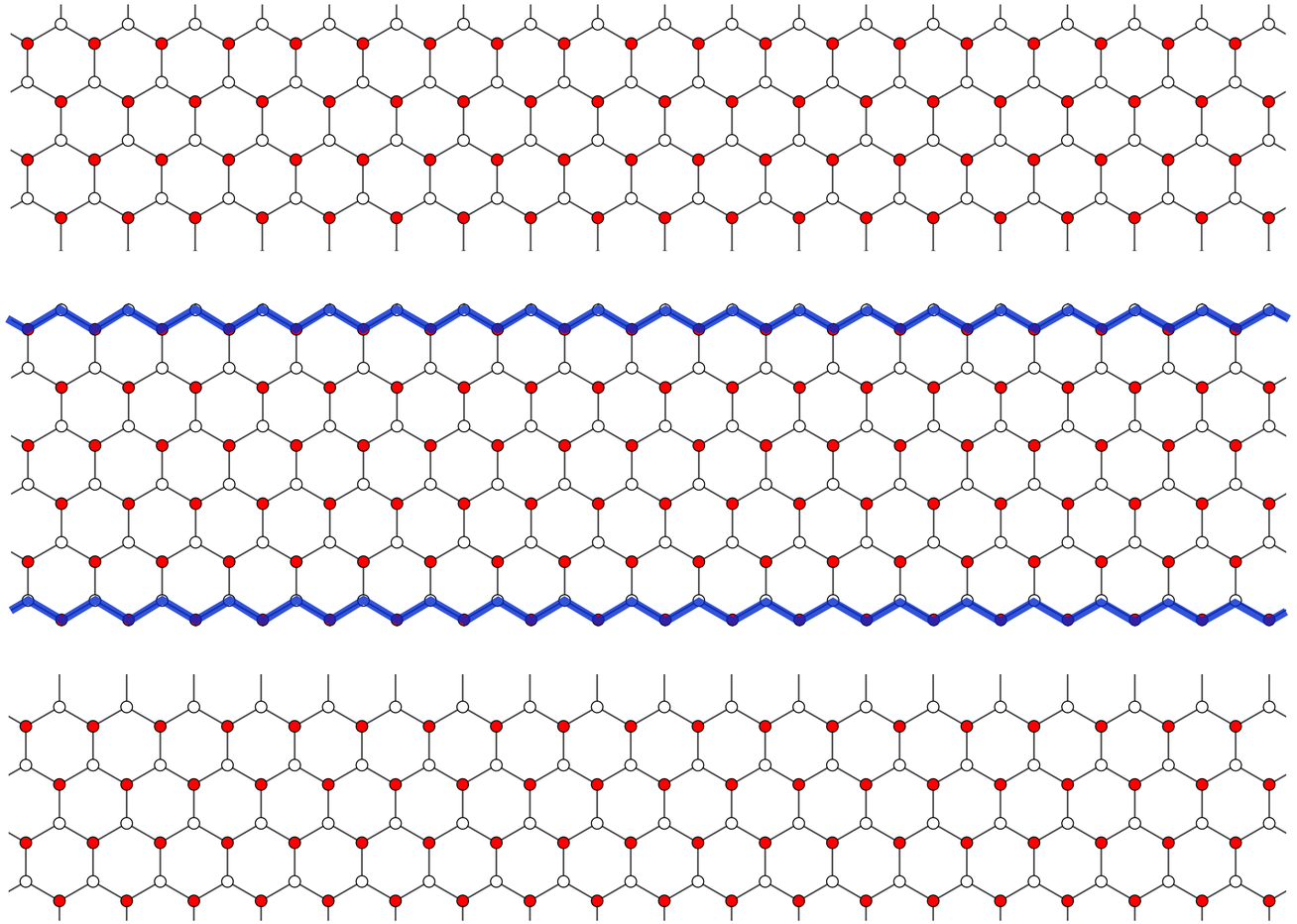

Tight-binding model

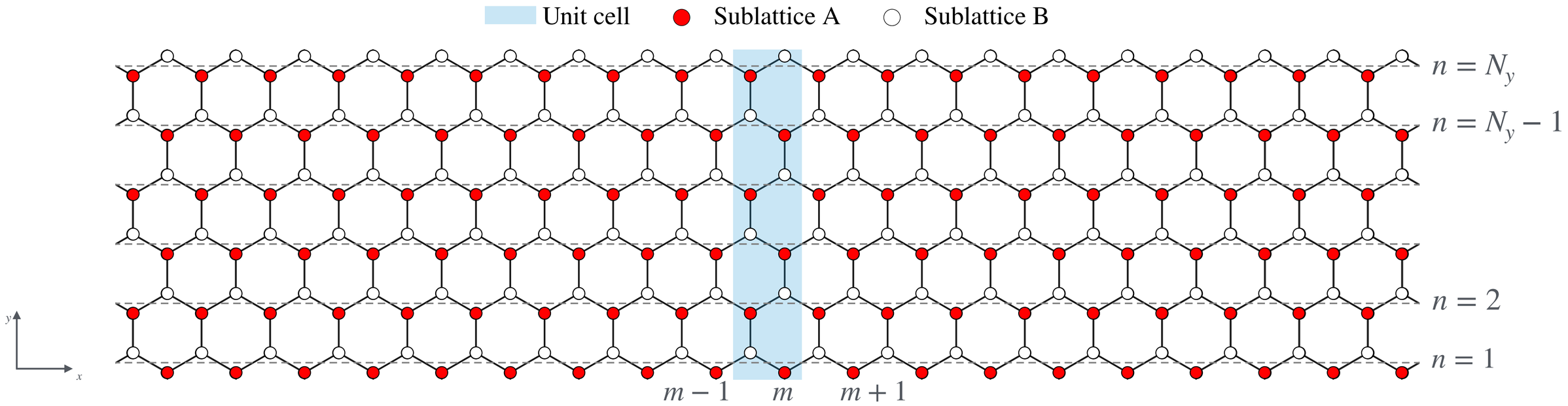

Tight-binding model

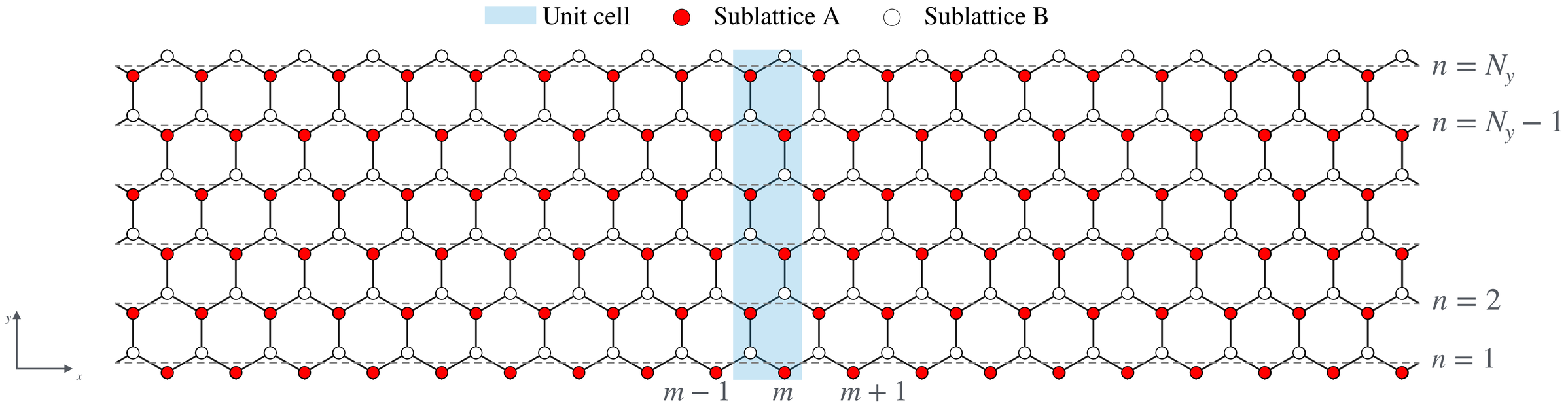

$$H_{\mathrm{tb}} = -t \sum_{\langle i,j \rangle, \sigma} \left(c_{i\sigma}^{\dagger} c_{j\sigma} + \mathrm{h.c.} \right)$$

Non-interacting band structure

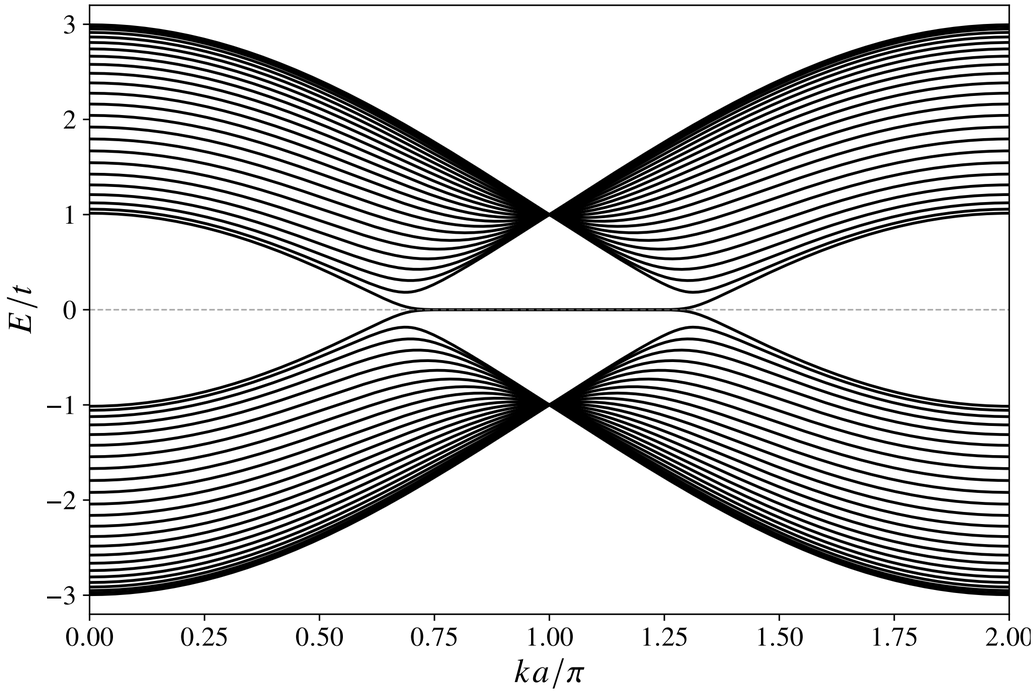

- Partially flat bands with edge localized states between Dirac points (edge states)
- Dispersive due to finite ribbon width

Non-interacting band structure

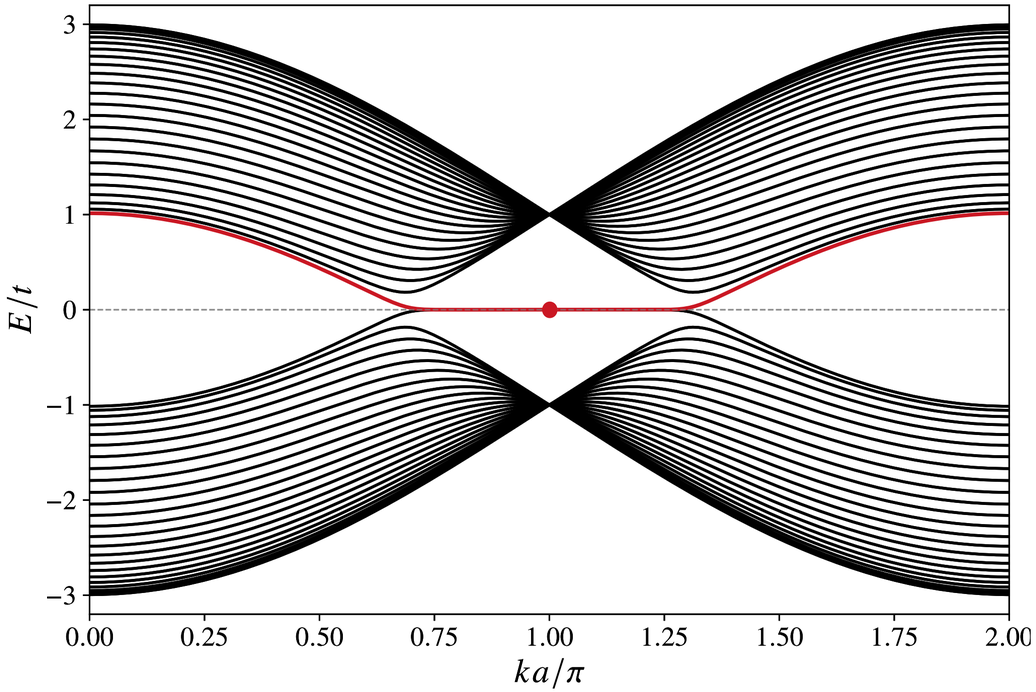

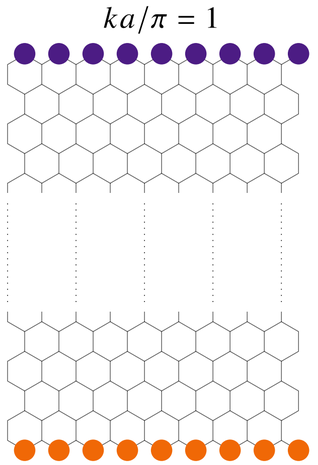

- Partially flat bands with edge localized states between Dirac points (edge states)
- Dispersive due to finite ribbon width
- Always degenerate bands and fully localized edge states at $k = \pi/a$

Non-interacting band structure

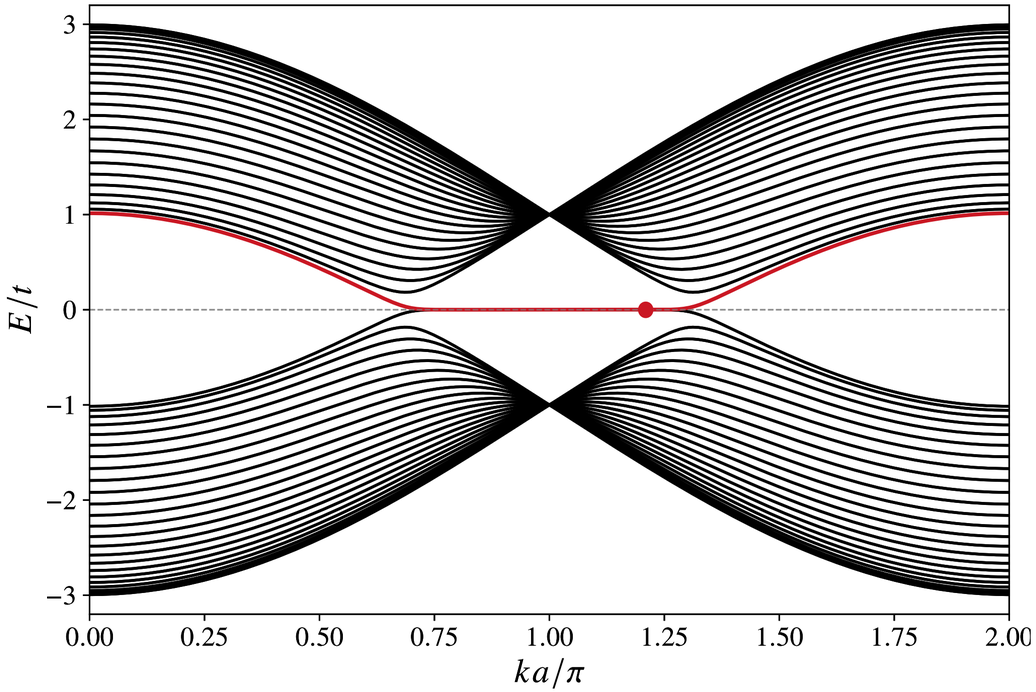

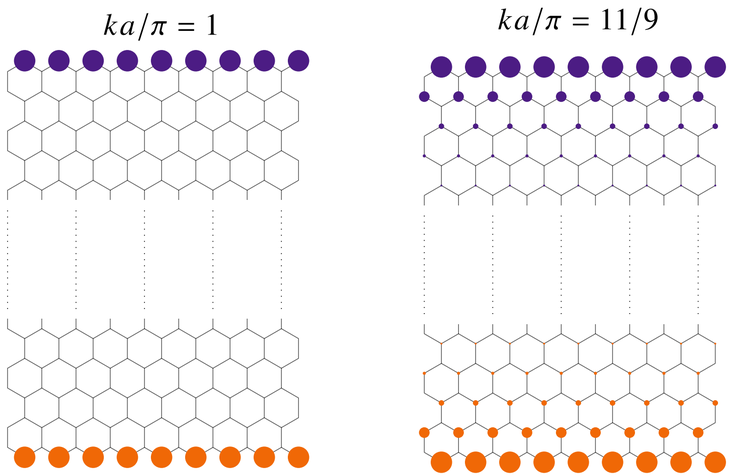

- Partially flat bands with edge localized states between Dirac points (edge states)
- Dispersive due to finite ribbon width
- Always degenerate bands and fully localized edge states at $k = \pi/a$

Non-interacting band structure

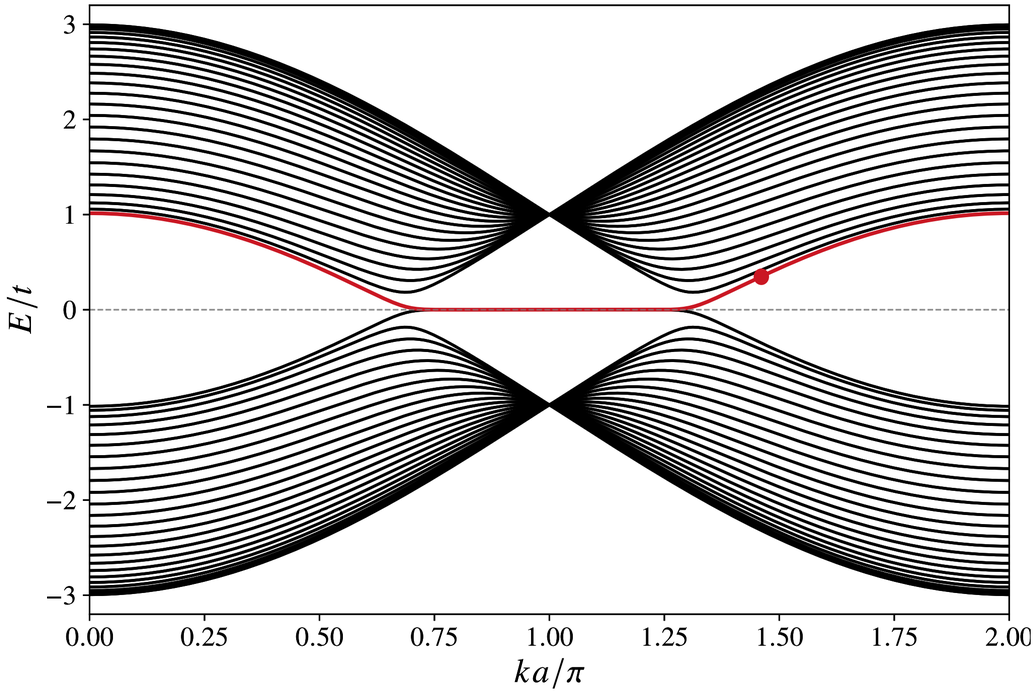

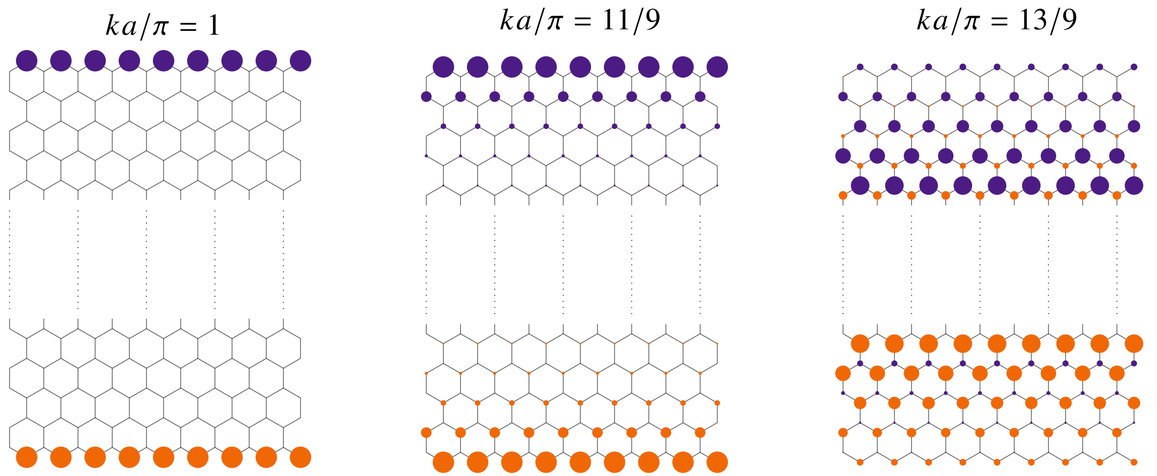

- Partially flat bands with edge localized states between Dirac points (edge states)
- Dispersive due to finite ribbon width
- Always degenerate bands and fully localized edge states at $k = \pi/a$

Hubbard model in mean-field approximation

- Introduce on-site interaction, governed by the on-site repulsion U

$$H = H_{\mathrm{tb}} + U \sum_i n_{i\uparrow} n_{i\downarrow}$$

- Mean-field Hubbard Hamiltonian

$$H_{\mathrm{mf}} = H_{\mathrm{tb}} + \frac{U}{2} \sum_{i,\sigma} \left(\langle n_i \rangle - \sigma \langle m_i \rangle \right) n_{i\sigma} + \frac{U}{4} \sum_i \left(\langle m_i \rangle^2 - \langle n_i \rangle^2 \right)$$

- Order parameters $\langle n_i \rangle = \langle n_{i\uparrow} \rangle + \langle n_{i\downarrow} \rangle$ and $\langle m_i \rangle = \langle n_{i\uparrow} \rangle - \langle n_{i\downarrow} \rangle$ are determined self-consistently

Magnetic order in zigzag nanoribbons

Antiferromagnetic (AF) order

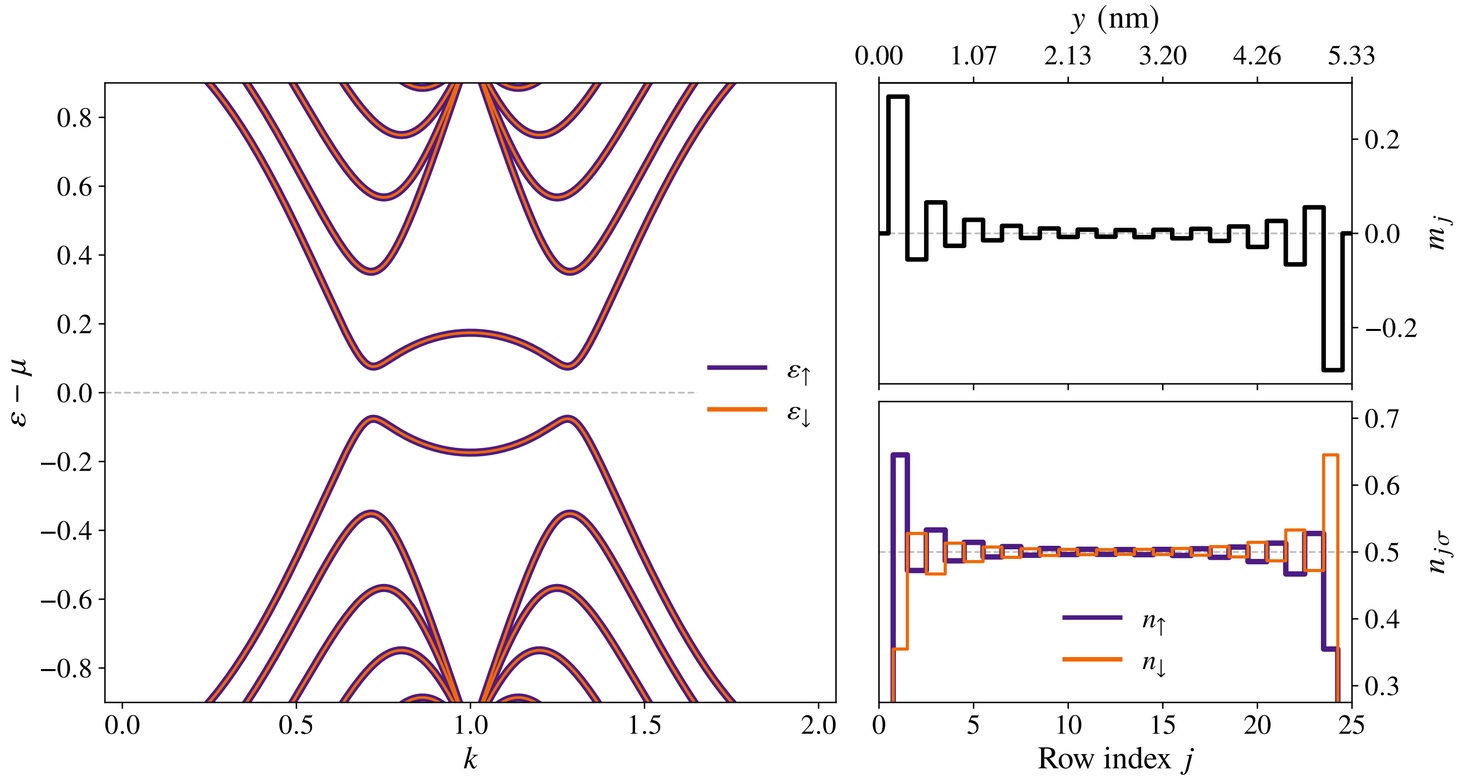

- Opposite spin orientation on the edges
- Spin-degenerate bands
- Interaction induced band gap

Ferromagnetic (F) order

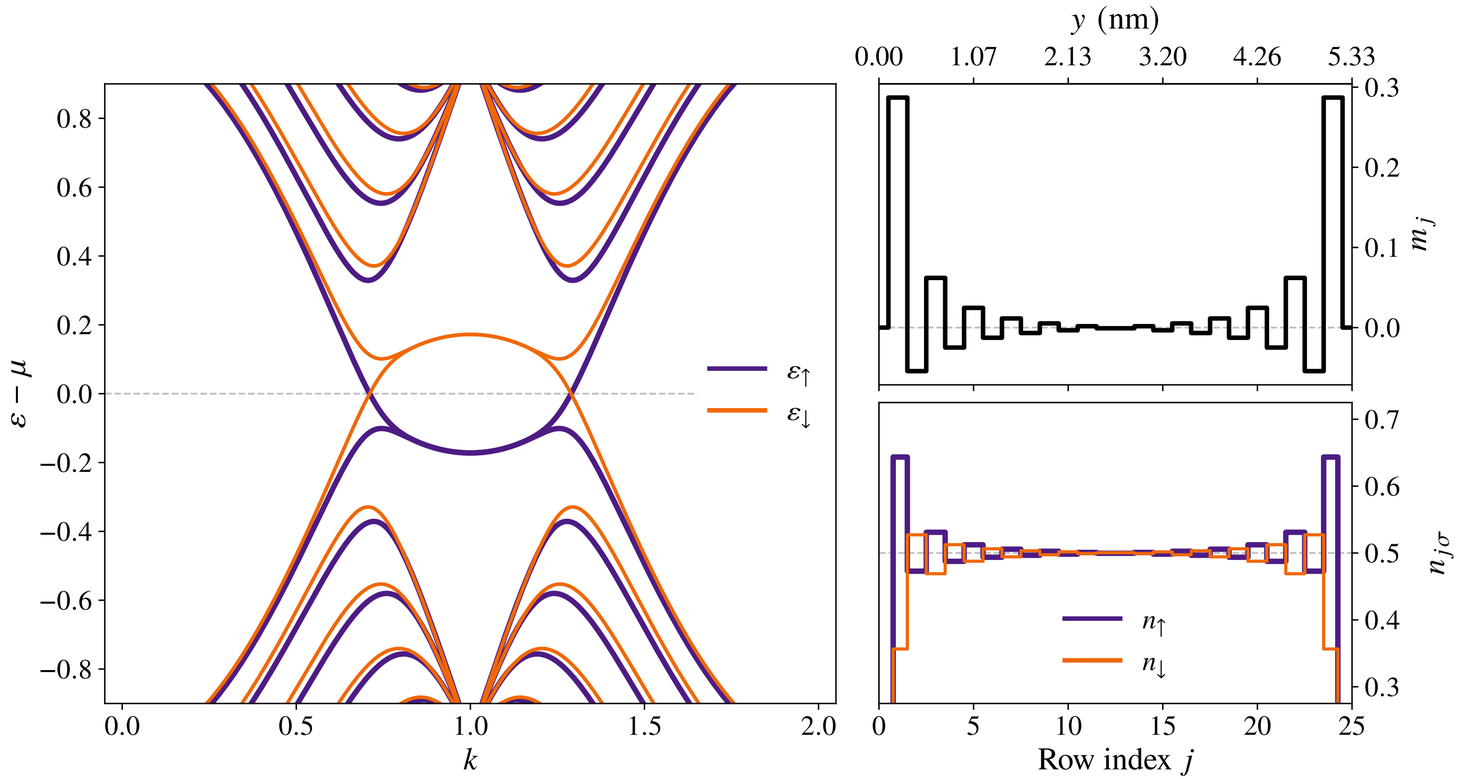

- Same spin orientation on both edges
- Spin-split bands
- Gapless band structure

Paramagnetic (P) order

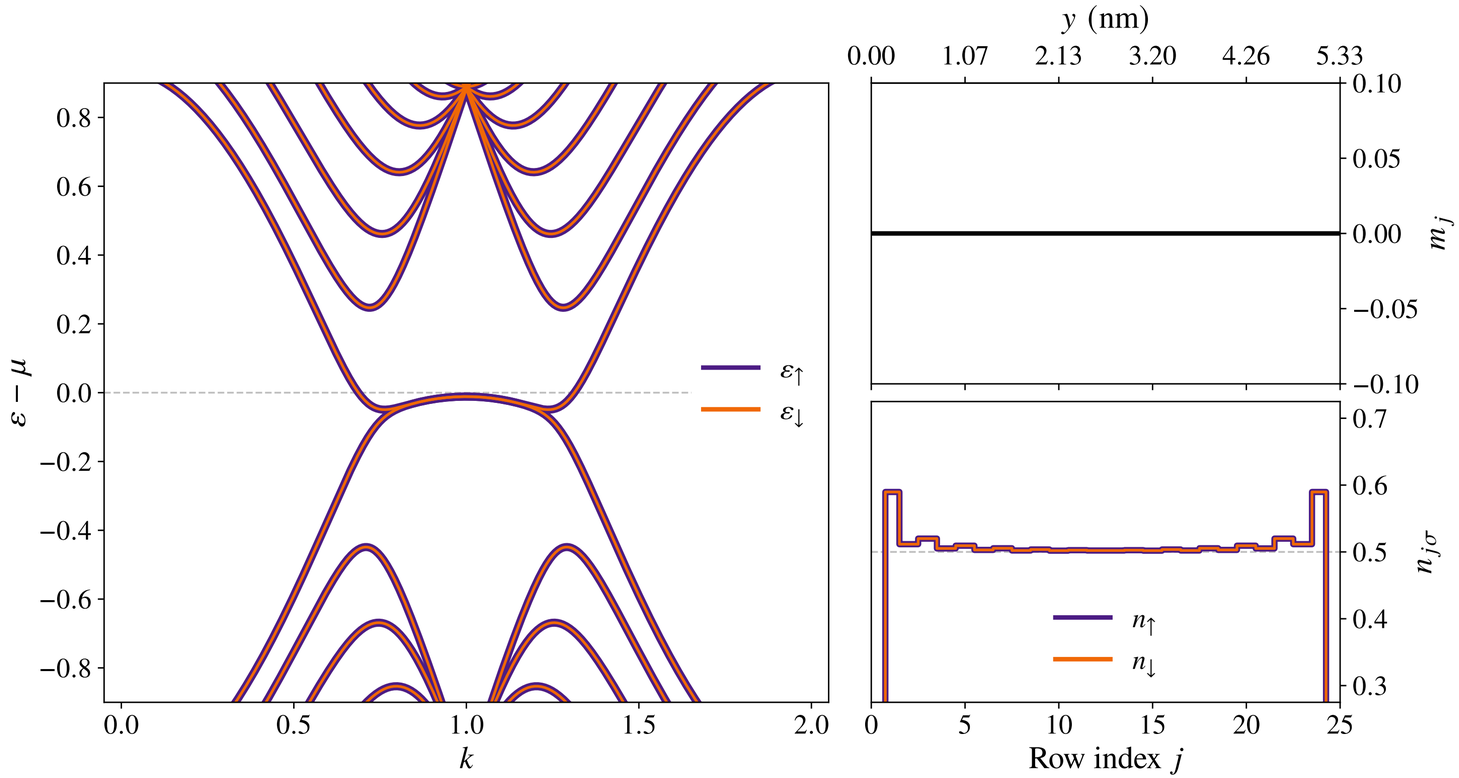

- All edge localized states completely filled
- Loss of magnetic order

Phase diagram

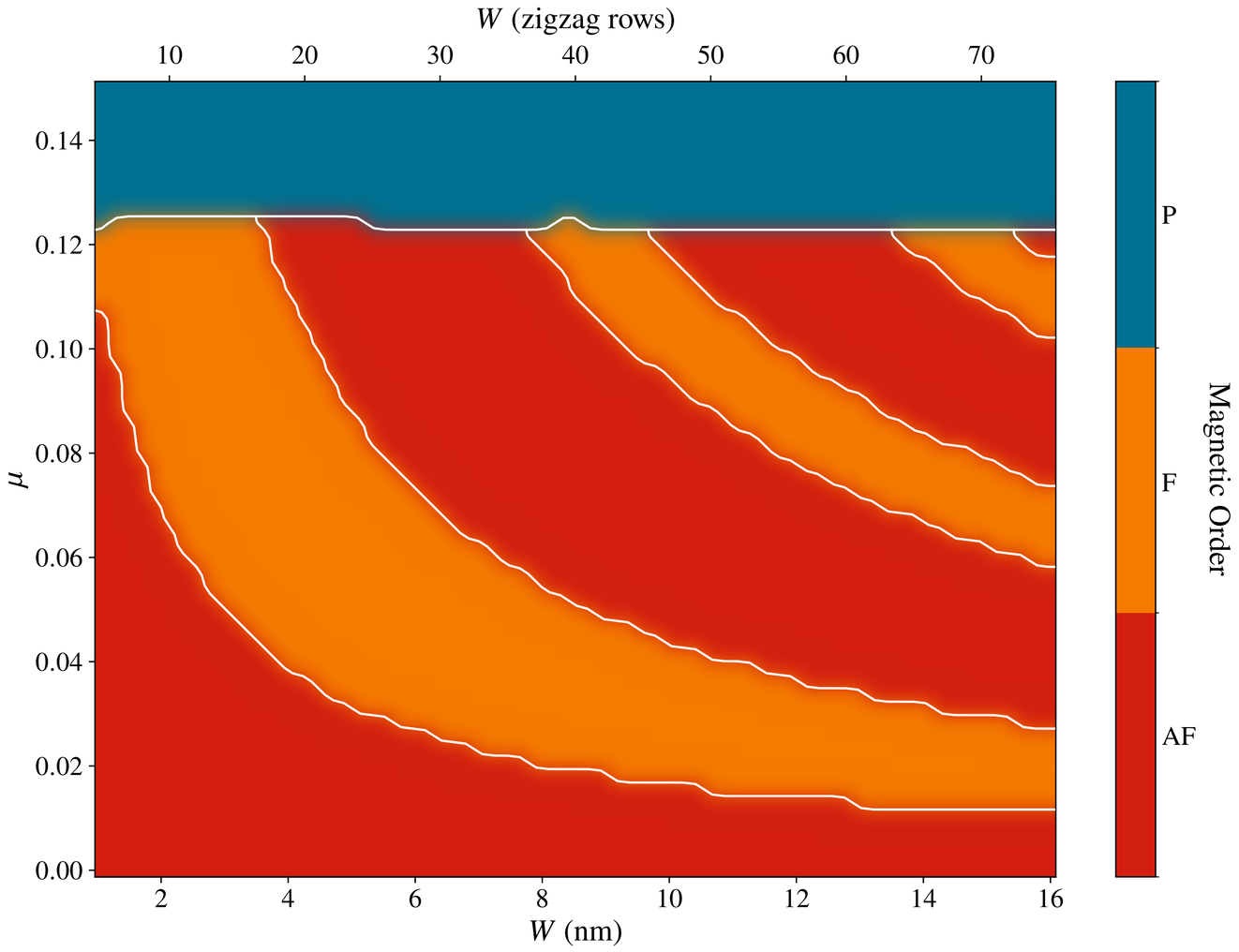

- $U = 1.2, T = 0.1\,\mathrm{K}$
- Smaller band gap and level spacing in wide ribbons
- Spectral overlap between bulk and edge bands
- Spin split bands in the F order accessible first

Path integral formalism and Hybrid Monte Carlo

Path integral formalism

- Partition function

$$Z = \mathrm{Tr} e^{-\beta(H-\mu N)}$$

Path integral formalism

- Partition function

$$Z = \mathrm{Tr} e^{-\beta(H-\mu N)}$$

- Decouple the interaction term via a Hubbard-Stratonovich transformation introducing auxiliary fields ϕ_{it}

Path integral formalism

- Partition function

$$Z = \mathrm{Tr} e^{-\beta(H-\mu N)}$$

- Decouple the interaction term via a Hubbard-Stratonovich transformation introducing auxiliary fields ϕ_{it}

- Partition function becomes functional integral over auxiliary fields

$$Z = \int \mathscr{D}[\phi] e^{-S[\phi]},$$

where the Hubbard action includes the fermion matrix $M_\sigma[\phi]$

$$S[\phi] = \sum_{it} \frac{\phi_{it}^2}{2\tilde{U}} - \log\det M_\uparrow[\phi] - \log\det M_\downarrow[\phi]$$

Path integral formalism

- Use Hybrid Monte Carlo (HMC) [Duane et al., Phys. Lett. B, 1987] to sample fields from

$$P[\phi] = \frac{1}{Z} e^{-S[\phi]}$$

- Two-point Green's function

$$C_{ij}(\tau) = \langle c_i(\tau) c_j^\dagger(0) \rangle = \lim_{N_{\mathrm{cf}} \to \infty} \frac{1}{N_{\mathrm{cf}}} \sum_n M^{-1}[\{\phi\}_n]_{i\tau, j0}$$

$$= \frac{1}{Z} \sum_{m,n} \langle m \,|\, c_{i\tau} \,|\, n \rangle \langle n \,|\, c_{j0}^\dagger \,|\, m \rangle e^{-\beta E_m} e^{-\tau(E_n - E_m)}$$

Energy extraction

- Momentum project the correlators

$$C_k(\tau)_{ml} = \sum_{ij} \phi^*_{kmi} C_{ij}(\tau) \phi_{klj}$$

- Extraction of interacting energies via the Truncated Hankel Correlator (THC) Method [Ostmeyer and Urbach, arXiv:2510.15500, 2025]

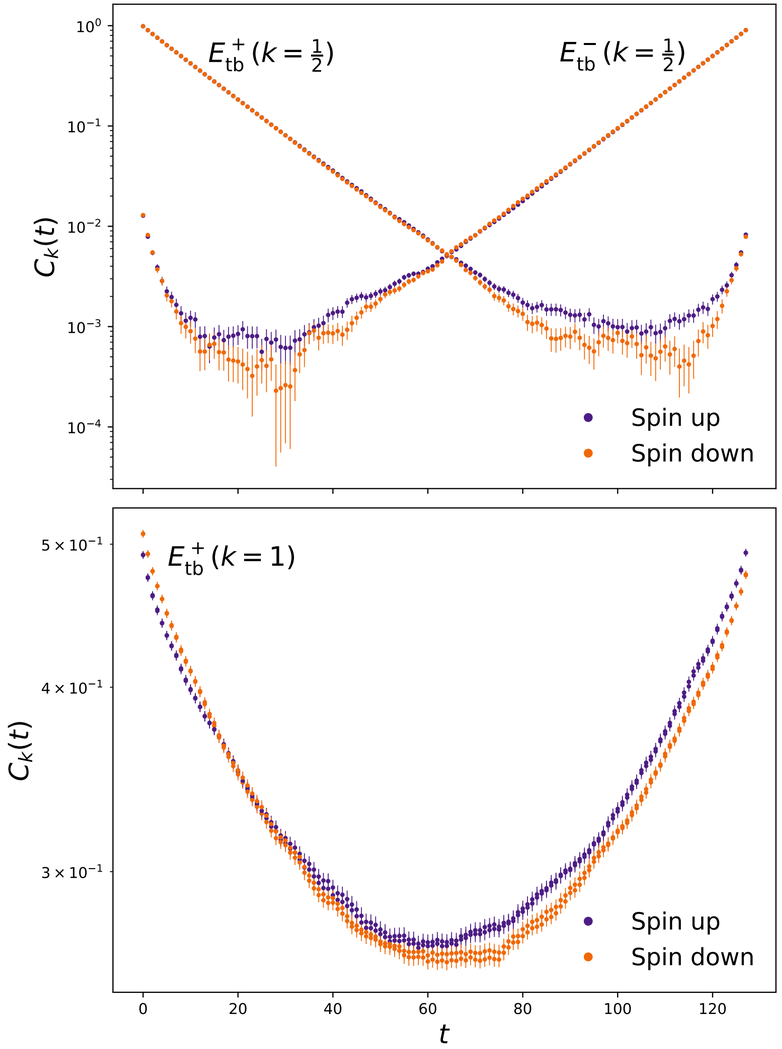

Comparison of spectra - Half-filling

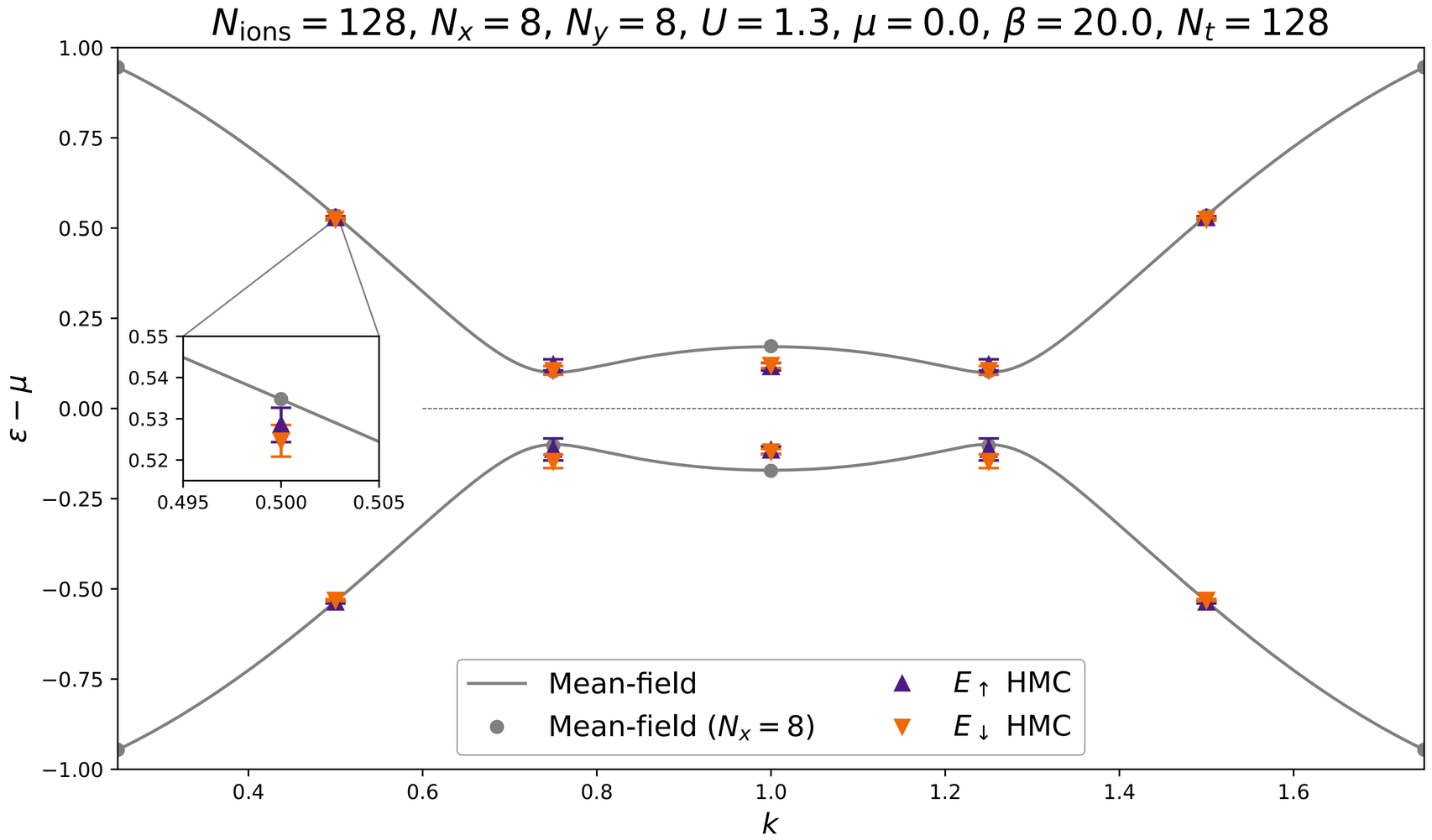

Finite chemical potential

- Mean-field theory predicts transition with increasing μ
- Identification of magnetic order from HMC simulation remains challenging
- Need additional observables as the spin-spin correlations between edges

$$\langle S^z_{it} S^z_{jt'} \rangle = \frac{1}{4} \sum_{\sigma\sigma'} \sigma\sigma' \langle c^\dagger_{it,\sigma} c_{it,\sigma} c^\dagger_{jt',\sigma'} c_{jt',\sigma'} \rangle$$

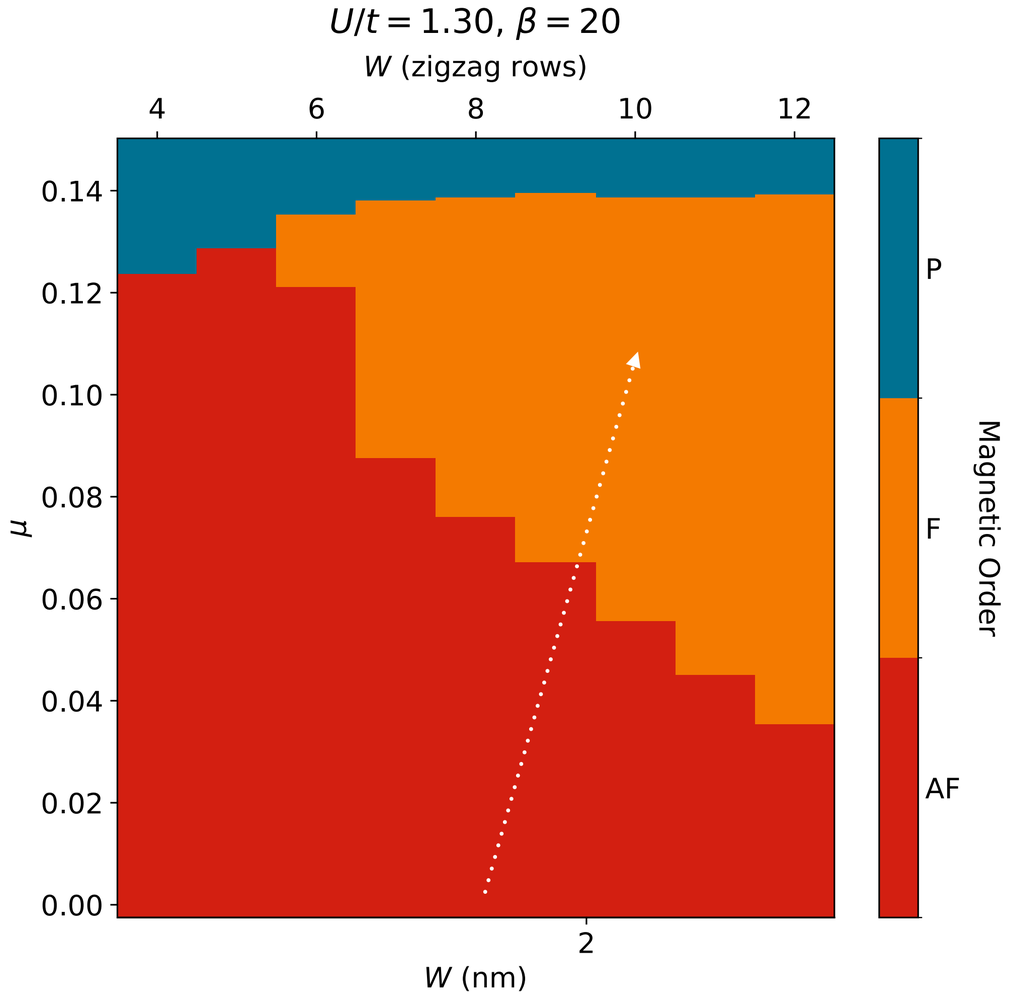

Non-zero chemical potential - Preliminary results

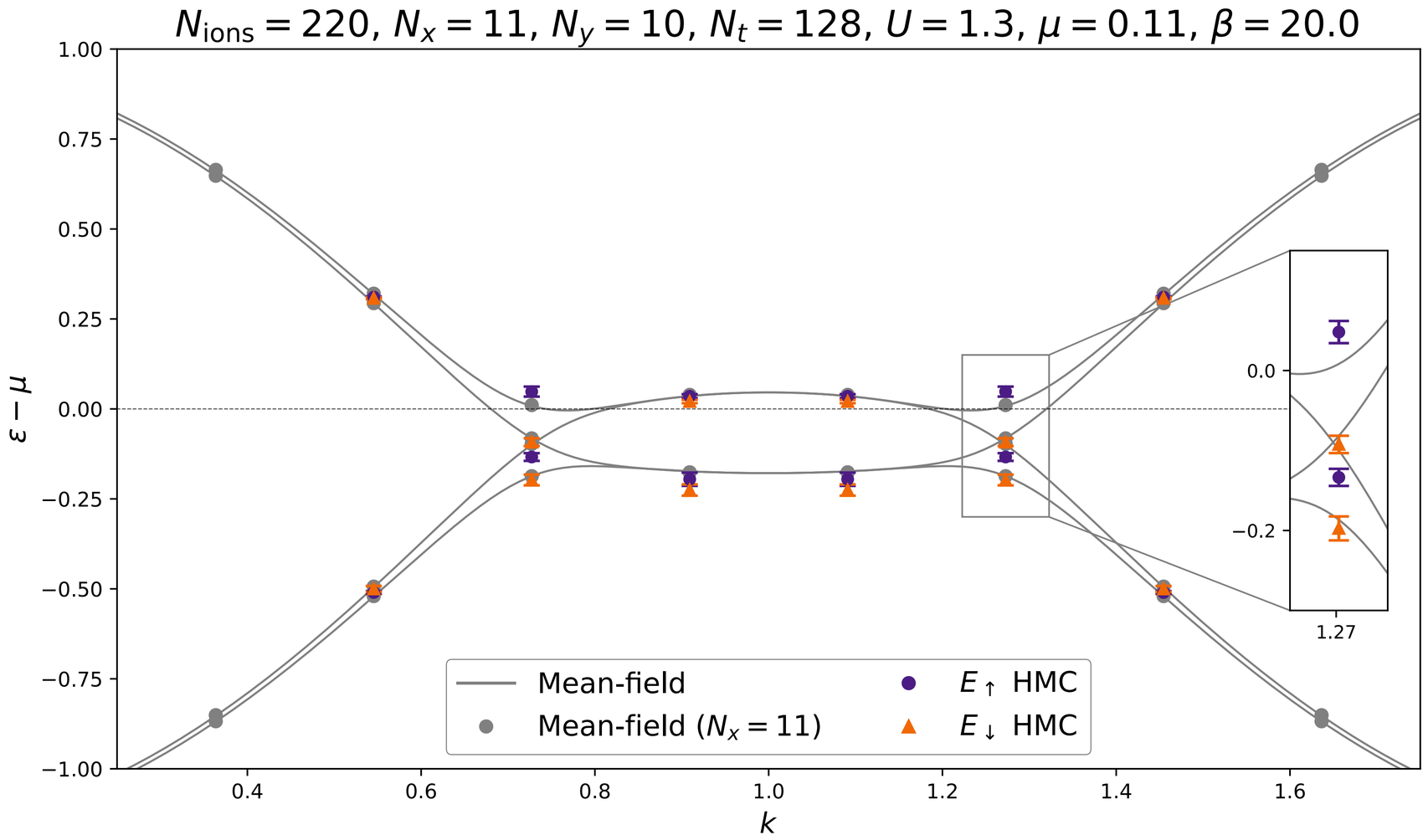

Non-zero chemical potential - Preliminary results

- Scalar parameter describing edge coupling

$$C_{\text{edges}} = \left\langle \sum_{\substack{i \in \text{top} \\ j \in \text{bottom}}} \eta_{ij} \vec{S}_i \vec{S}_j \right\rangle = \begin{cases} < 0 & \text{AF} \\ > 0 & \text{F} \end{cases}, \qquad \eta_{ij} = \pm 1$$

- $N_x = 8, N_y = 8, \mu = 0.00$: $C_{\text{edges}} = -0.0455 \pm 0.0016$

  $N_x = 11, N_y = 10, \mu = 0.11$: $C_{\text{edges}} = 0.0066 \pm 0.0004$

Conclusion

- Systematic study of the magnetic order depending on chemical potential and width
- Additional phase transition in wide ribbons
- Validation of mean-field results with HMC simulations at half-filling and evidence of transition at finite μ

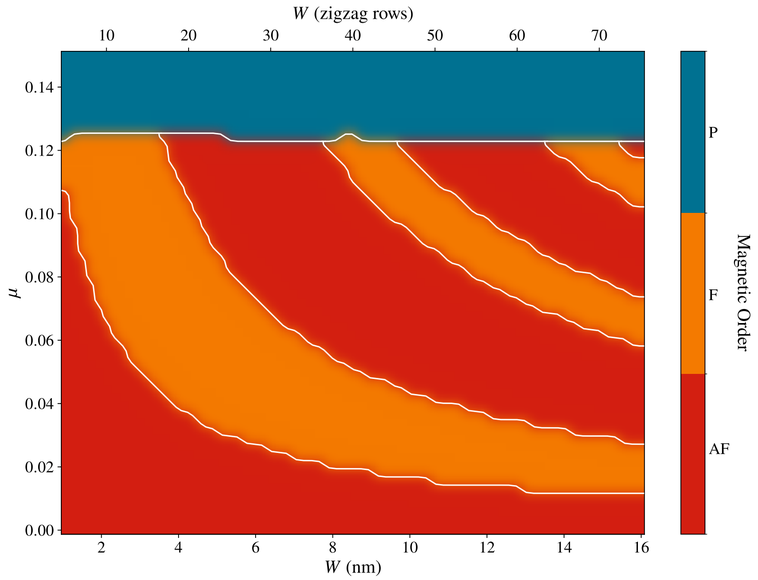

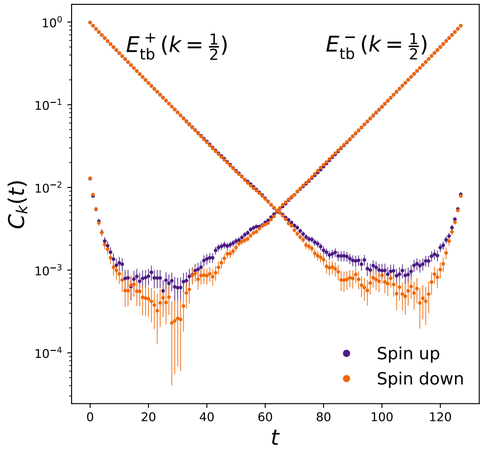

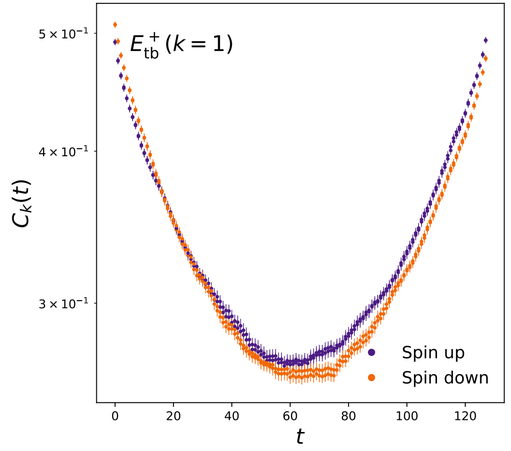

Outlook

- Validation of magnetic phase transition in narrow ribbons at finite μ
- Further examine the competition between edge and bulk states

With special thanks to

Lin Wang

Tom Luu

JÜLICH
Forschungszentrum

Backup slides

Non-zero chemical potential

- Zigzag ribbon at $n_x = 11$, $n_y = 10$, $\mu = 0.11$, $U = 1.3$ and $\beta = 20$
- Mean-field predicts F order

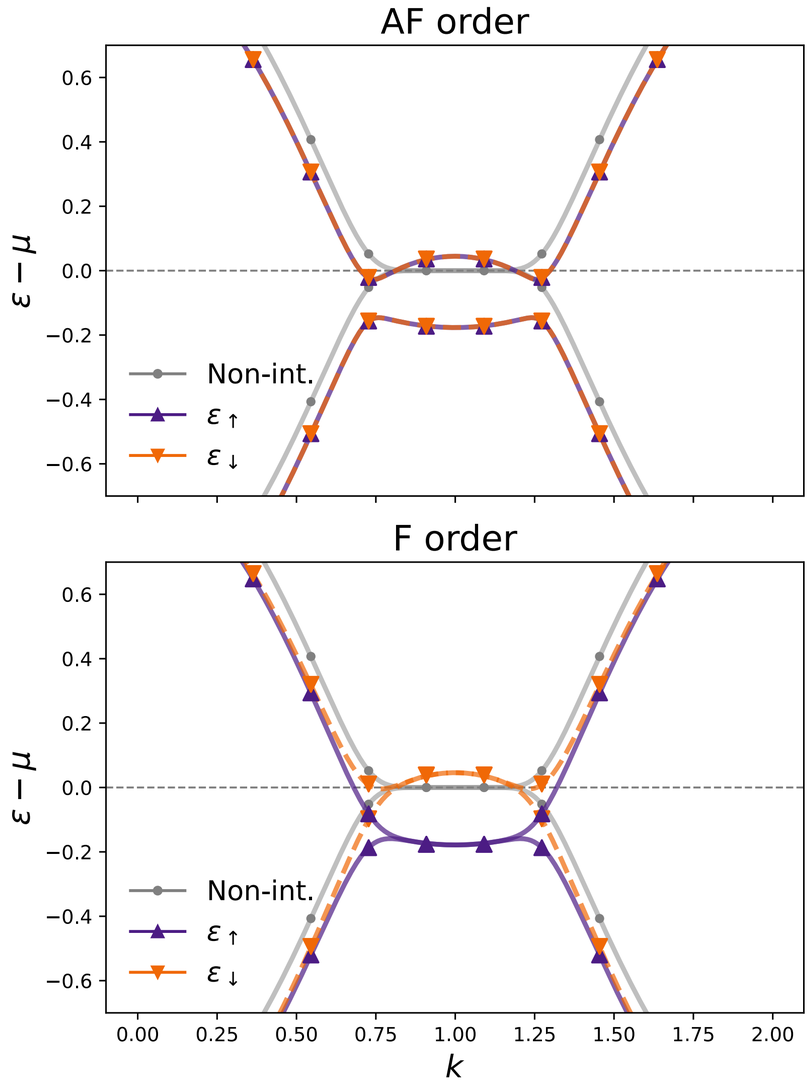

Non-zero chemical potential - Preliminary Results

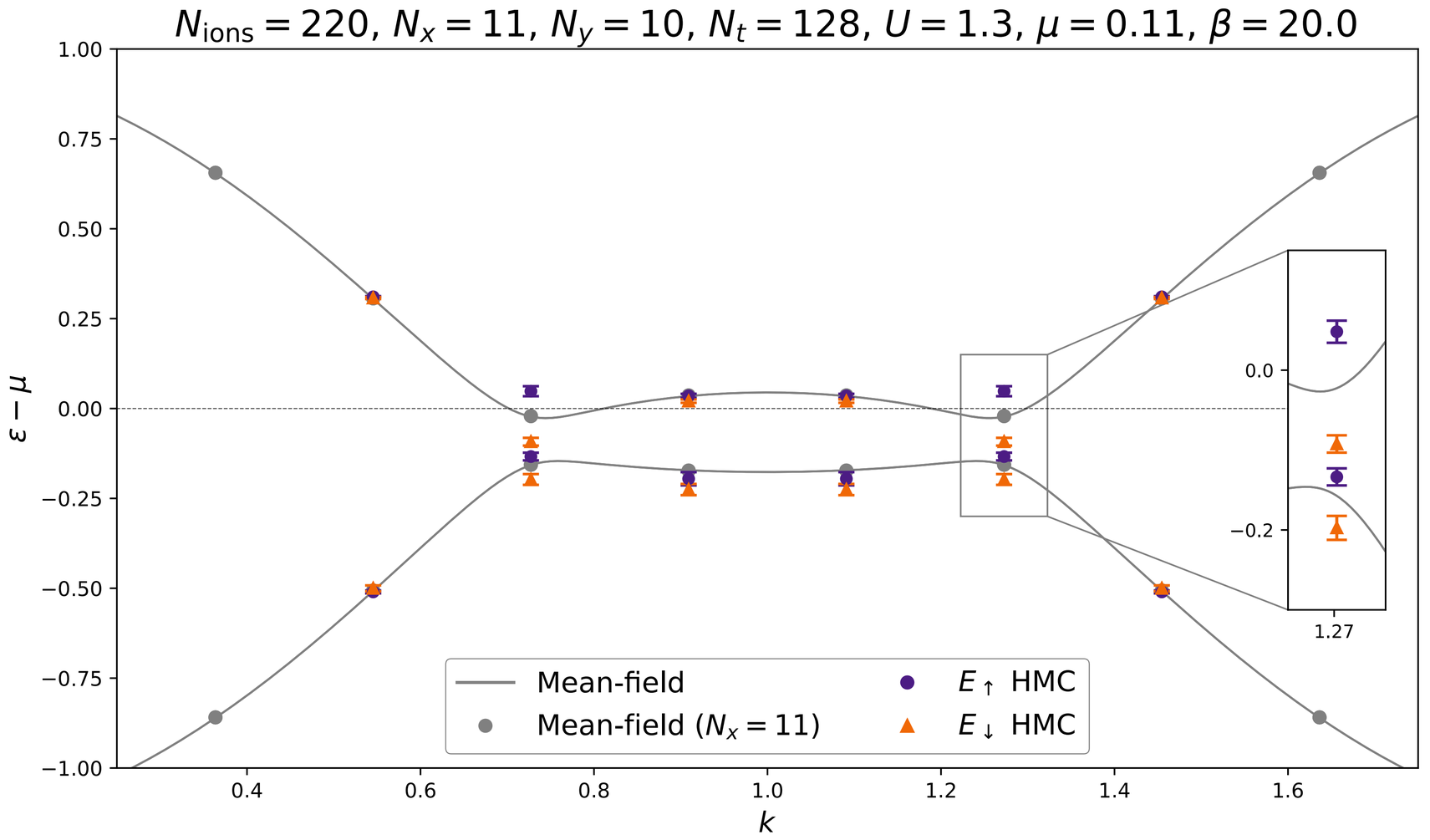

Fermion matrix

$$M_\sigma[\phi]_{it,jt'} = \delta_{ij}\delta_{t,t'} - s_t \left[e^{\tilde{\kappa}-\tilde{\mu}\mathrm{I}\mp\sigma\phi_t}\right]_{ij} \delta_{t,t'+1} \,.$$

Tight-binding Model

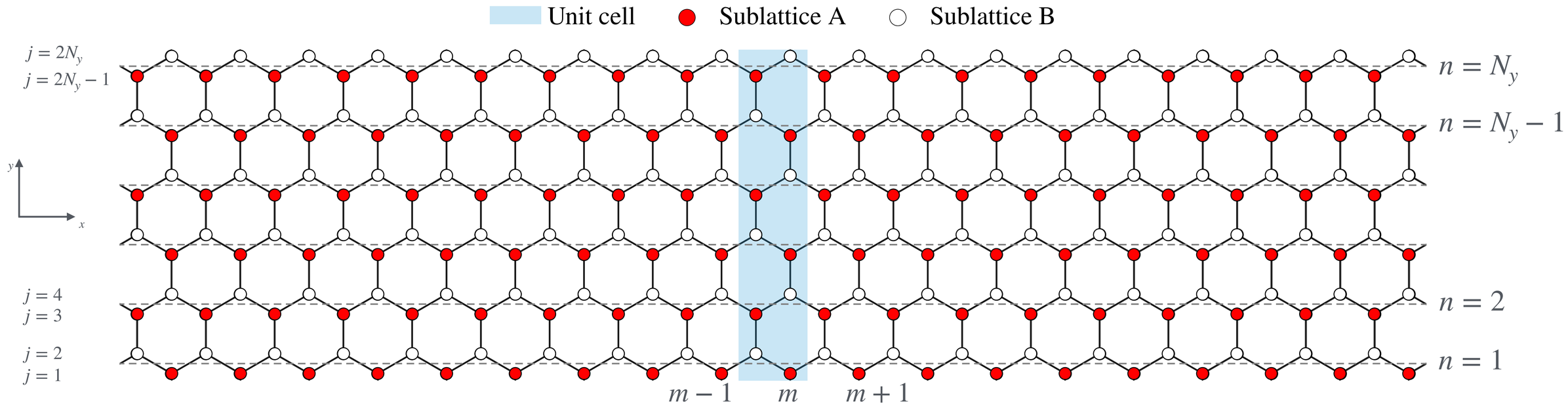

$$H_{\text{tb}} = -t \sum_{m,n,\sigma} \left\{ a_\sigma^\dagger(m,n) b_\sigma(m,n) + a_\sigma^\dagger(m,n) b_\sigma(m,n-1) + a_\sigma^\dagger(m,n) b_\sigma(m-1,n) + \text{h.c.} \right\}$$

Periodic boundary conditions →

$$H_{\text{tb}} = -t \sum_{k,n,\sigma} \left\{ \left(1 + e^{-ika}\right) a_\sigma^\dagger(k,n) b_\sigma(k,n) + a_\sigma^\dagger(k,n) b_\sigma(k,n-1) + \text{h.c.} \right\}$$

Narrow ribbon

$W = 5.33\,\mathrm{nm}$

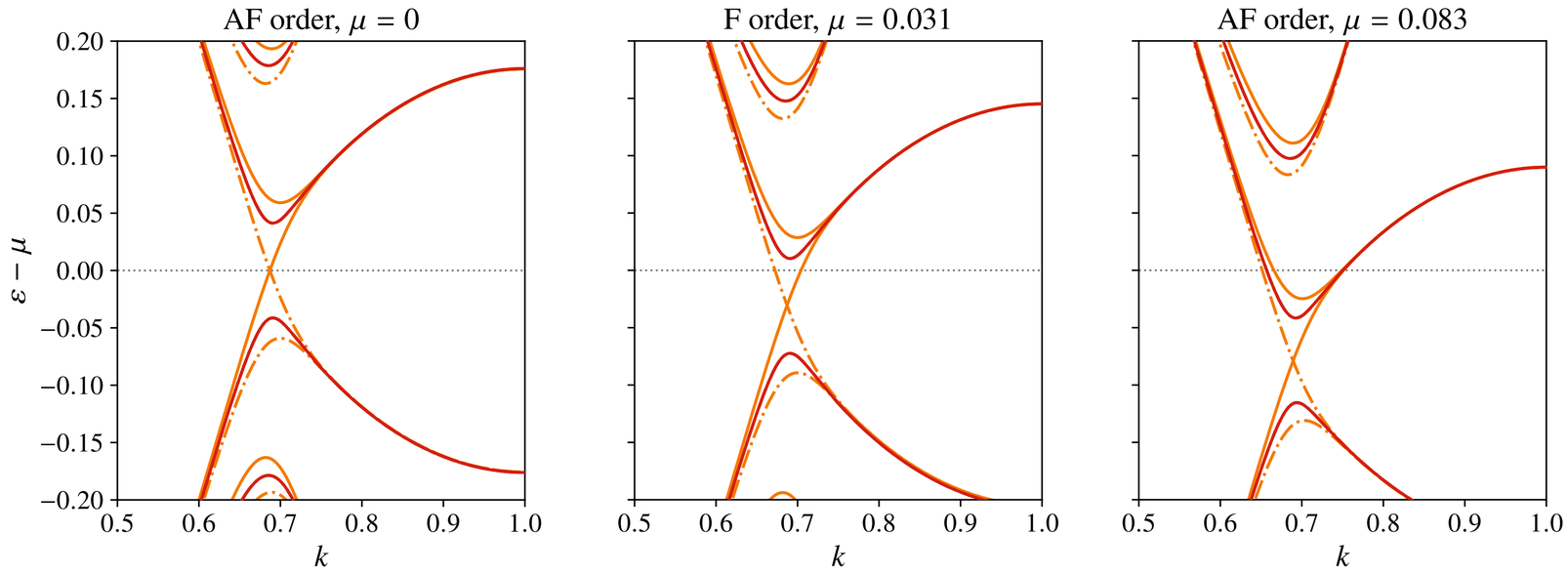

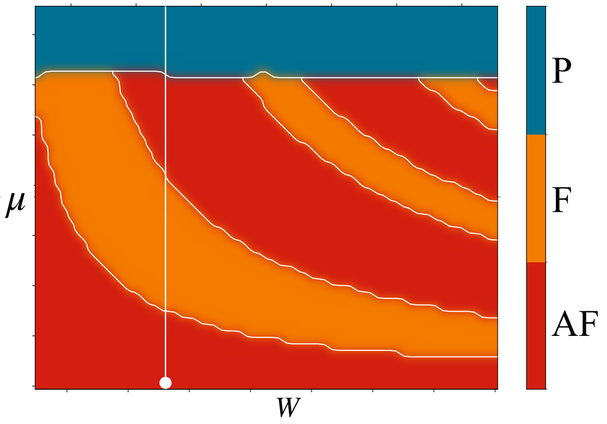

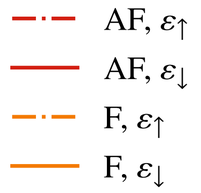

- Only edge bands contribute
- Additional filling in F order compared to AF order

Band structure

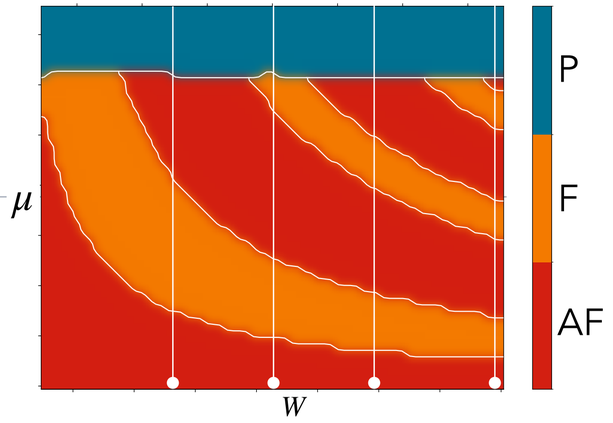

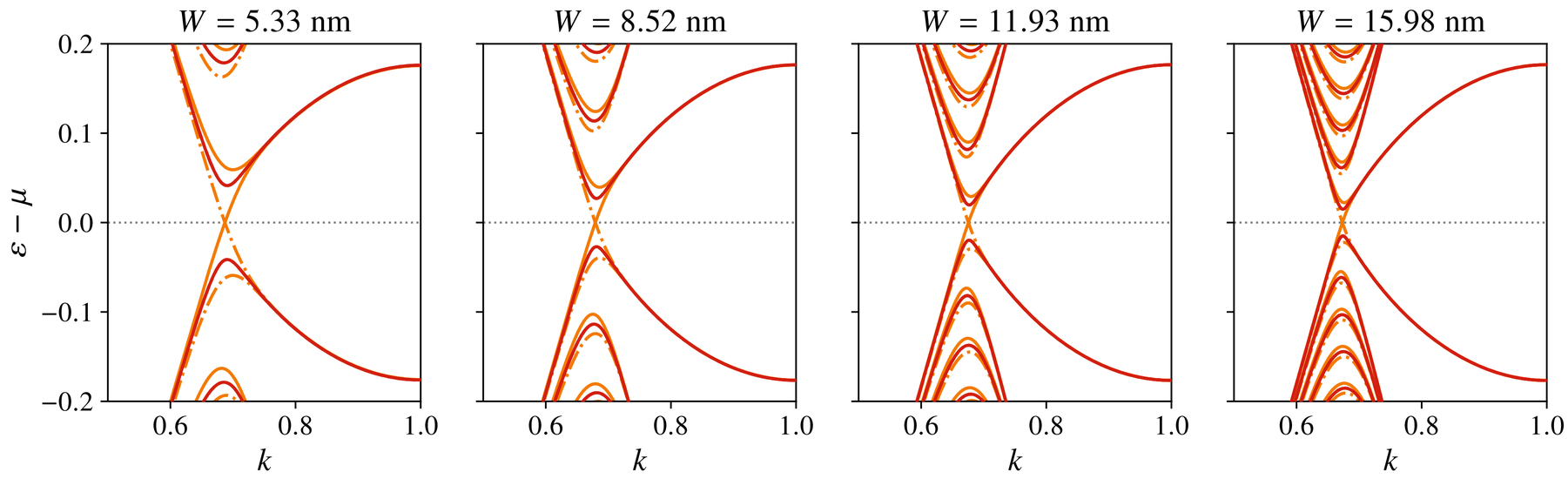

- Smaller band gap and level spacing in wide ribbons
- Spin split bands in the F order accessible first
- Spectral overlap between bulk and edge bands

Wide ribbon

$W = 11.93\,\mathrm{nm}$

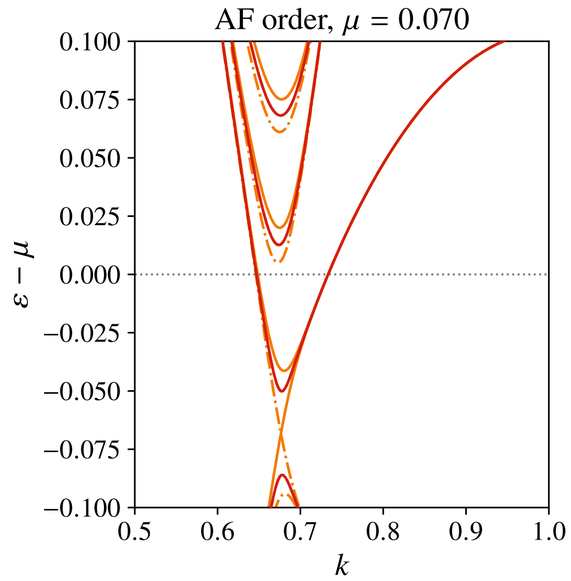

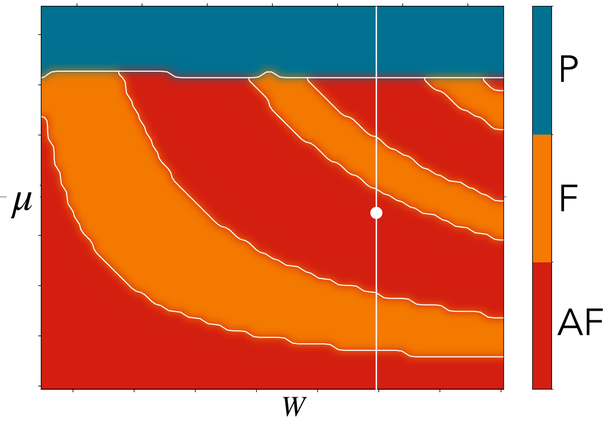

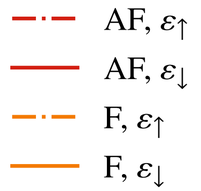

- Contribution from bulk states
- Occupation of states in F order at bulk band minimum

Wide ribbon

$W = 11.93\,\mathrm{nm}$

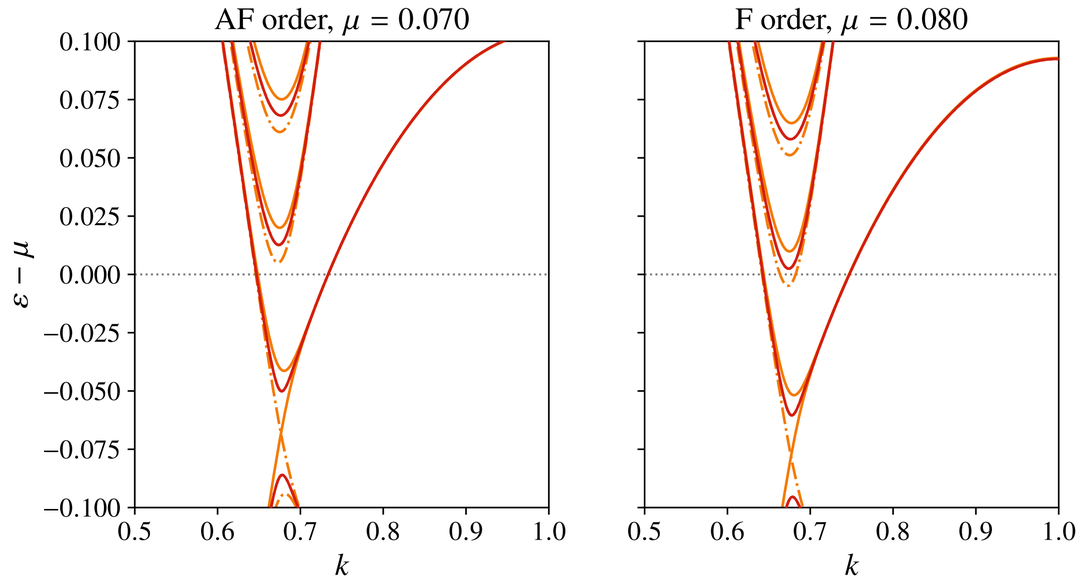

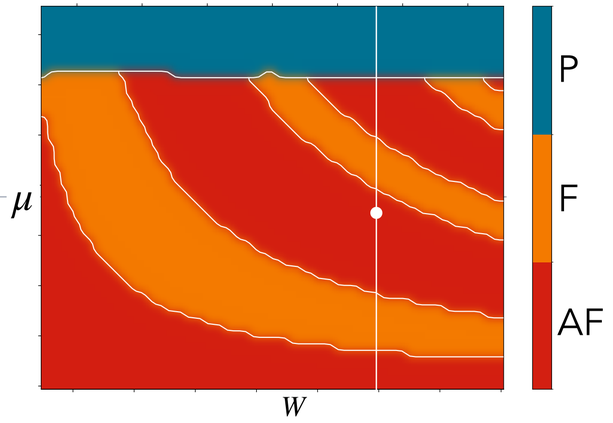

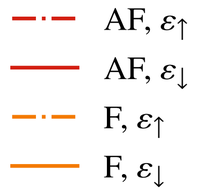

- Contribution from bulk states
- Occupation of states in F order at bulk band minimum

Wide ribbon

$W = 11.93\,\mathrm{nm}$

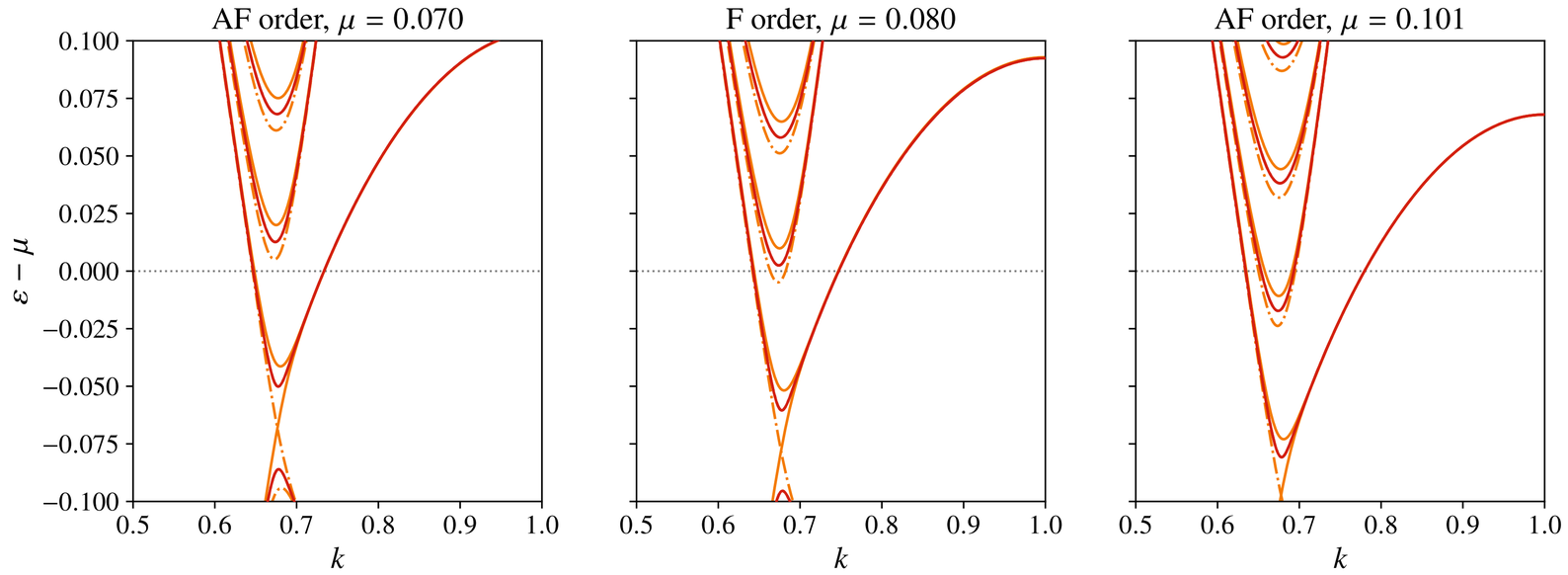

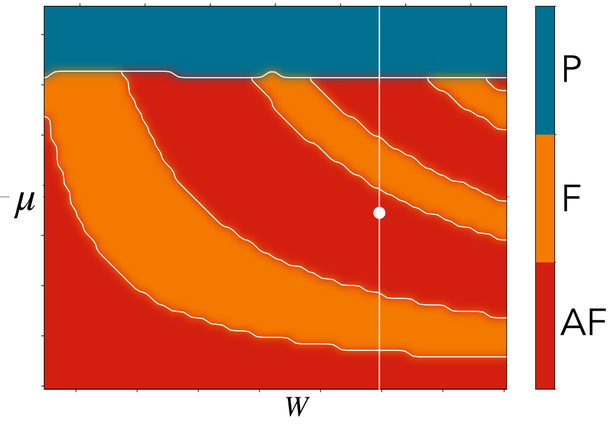

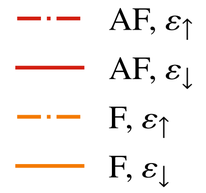

- Contribution from bulk states
- Occupation of states in F order at bulk band minimum

Trial density matrix $\boldsymbol{\rho}$

- Mean-field trial density matrix

$$\rho = \frac{1}{Z_\rho} e^{-\beta(H_{\mathrm{tb}} - \mu N + \sum_i \omega_i n_i + \sum_i \lambda_i m_i)} \equiv \frac{1}{Z_\rho} e^{-\beta K}$$

- Elimination of the conjugate fields ω_i and λ_i from stationarity of Ω_ρ

$$\omega_i = \frac{U}{2} \bar{n}_i \quad \text{and} \quad \lambda_i = -\frac{U}{2} \bar{m}_i,$$

where $\bar{x}_i \equiv \bar{x}_i^t = \langle x_i \rangle^{t-1}$ for $x = n, m$

Variational mean-field theory

- For a given trial density matrix ρ define the variational grand potential functional Ω_ρ by

$$\Omega \leq \Omega_\rho = \langle H - \mu N \rangle_\rho + \frac{1}{\beta} \langle \ln \rho \rangle_\rho$$

- Stationarity w.r.t. the densities yields self-consistent mean-field equations

$$\langle n_j \rangle = \frac{1}{N_x} \sum_{nk\sigma} f(\varepsilon_{nk\sigma} - \mu; \beta) \, |\psi_{nk\sigma}(j)|^2 = \langle n_{j\uparrow} \rangle + \langle n_{j\downarrow} \rangle$$

$$\langle m_j \rangle = \frac{1}{N_x} \sum_{nk\sigma} \sigma f(\varepsilon_{nk\sigma} - \mu; \beta) \, |\psi_{nk\sigma}(j)|^2 = \langle n_{j\uparrow} \rangle - \langle n_{j\downarrow} \rangle$$

[Chaikin & Lubensky, *Principles of Condensed Matter Physics*, Cambridge University Press, 1995; Shi, arXiv:1901.10844, 2019]

Self-consistent mean-field solutions

$$\langle n_j \rangle^{(t+1)} = \frac{1}{N_x} \sum_{nk\sigma} f(\varepsilon^{(t)}_{nk\sigma} - \mu; \beta) \, |\psi^{(t)}_{nk\sigma}(j)|^2 = \langle n_{j\uparrow} \rangle^{(t+1)} + \langle n_{j\downarrow} \rangle^{(t+1)}$$

$$\langle m_j \rangle^{(t+1)} = \frac{1}{N_x} \sum_{nk\sigma} \sigma f(\varepsilon^{(t)}_{nk\sigma} - \mu; \beta) \, |\psi^{(t)}_{nk\sigma}(j)|^2 = \langle n_{j\uparrow} \rangle^{(t+1)} - \langle n_{j\downarrow} \rangle^{(t+1)}$$

- Solve fixed point problem by iterative updates
- Density inputs at step $t + 1$ are estimates from self-consistent equations at step t
- For ground state selection: Choose self-consistent mean-field solution with lowest Ω_ρ

Fb order

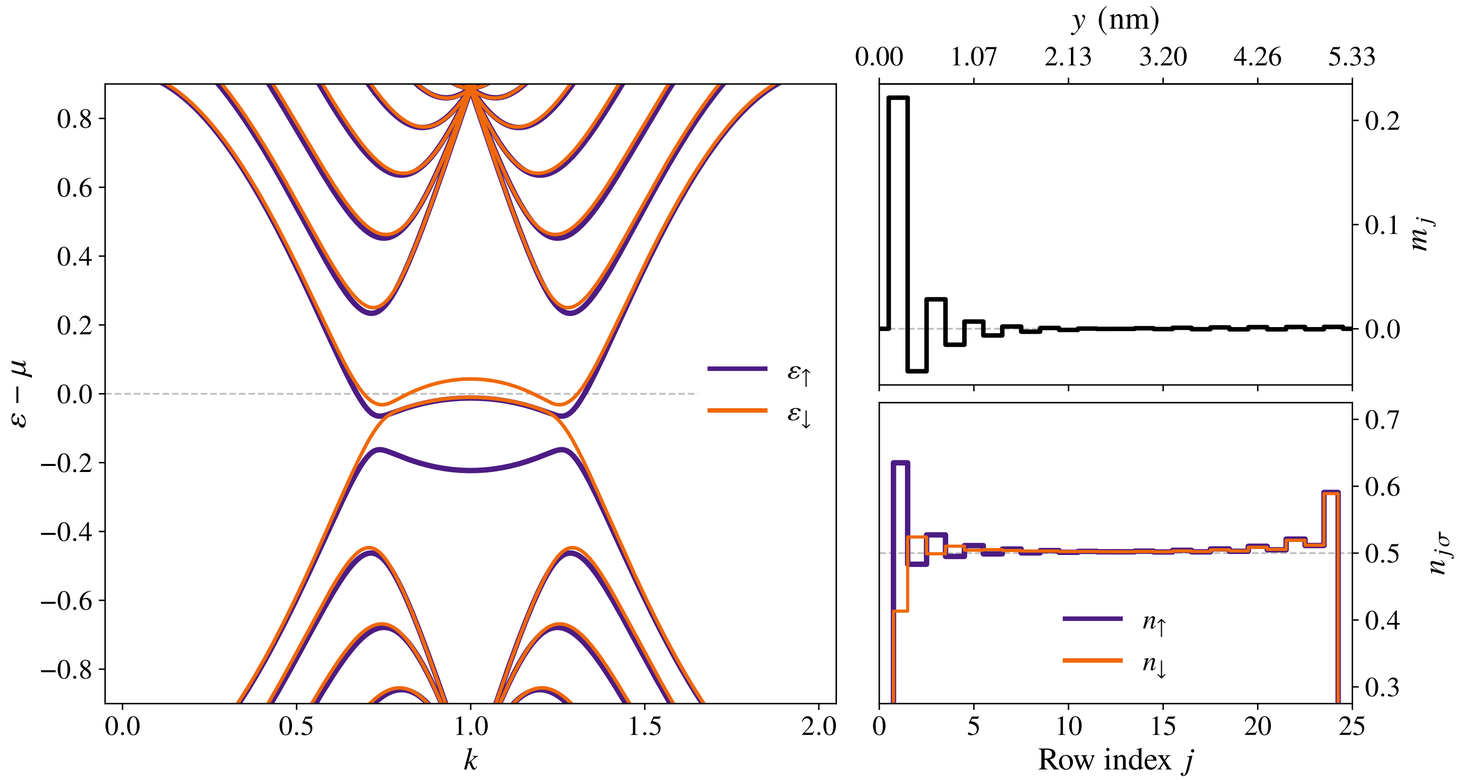

- Solution at sufficiently large doping
- Broken charge symmetry
- AF and F order band characteristics

Phase diagram (discrete)

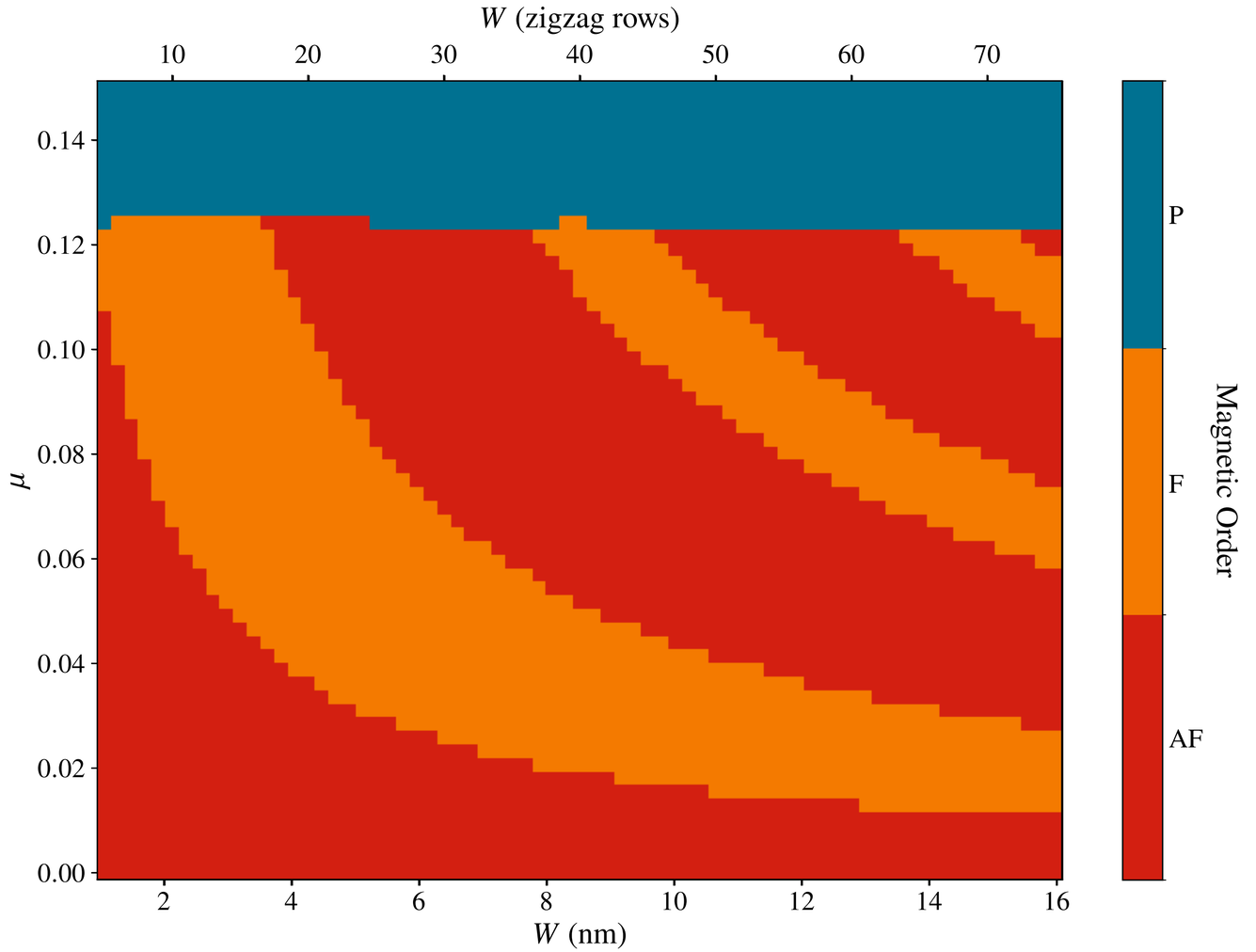

$U/t = 1.2$

$T = 0.1\,\mathrm{K}$

Phase diagram at fixed doping

$$\delta n = \frac{N_{\mathrm{el}} - N_{\mathrm{sites}}}{N_x}$$

$$U/t = 1.2,\ T = 0.1\,\mathrm{K}$$

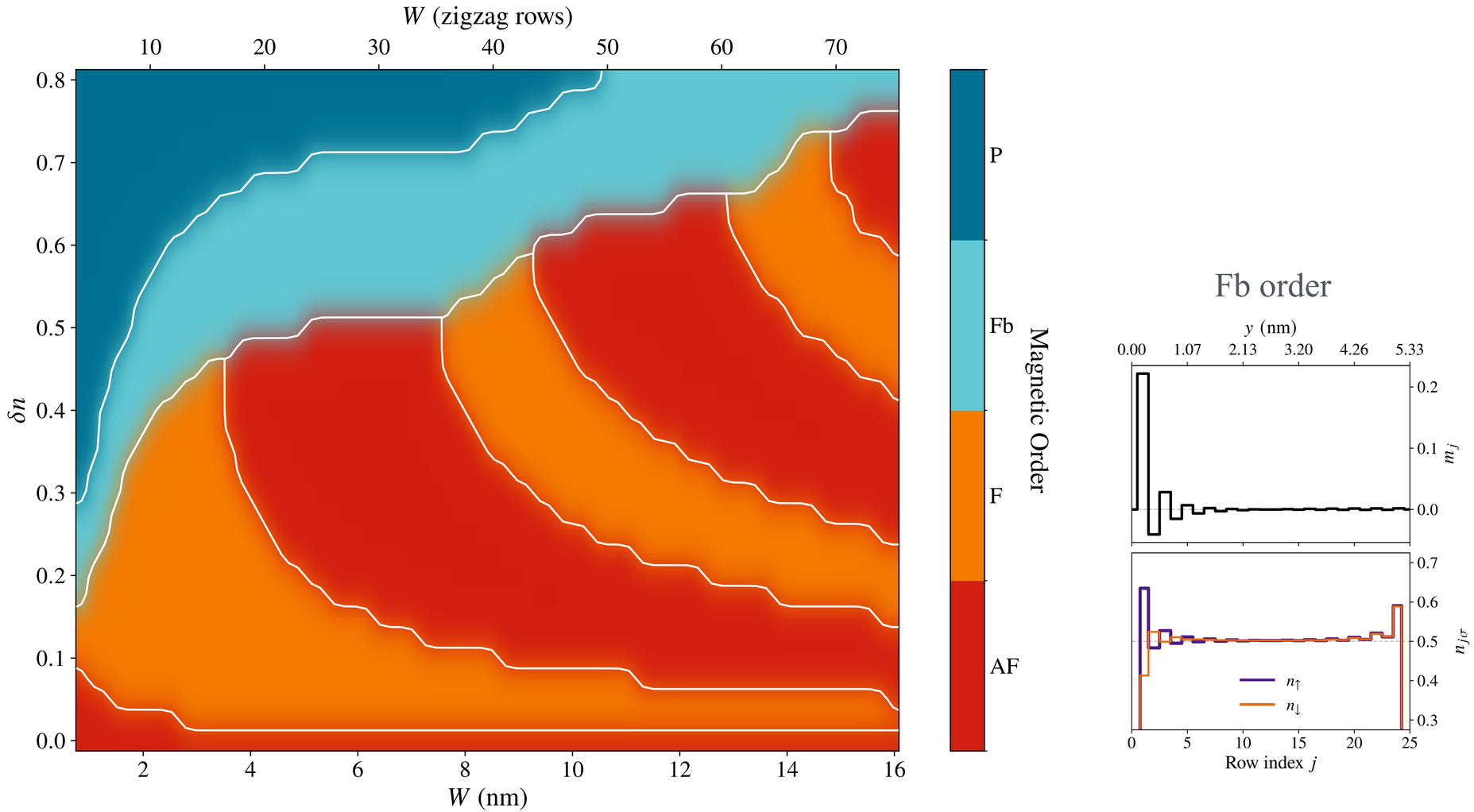

Phase diagram at fixed doping (discrete)

$$\delta n = \frac{N_{\mathrm{el}} - N_{\mathrm{sites}}}{N_x}$$

$U/t = 1.2,\ T = 0.1\,\mathrm{K}$

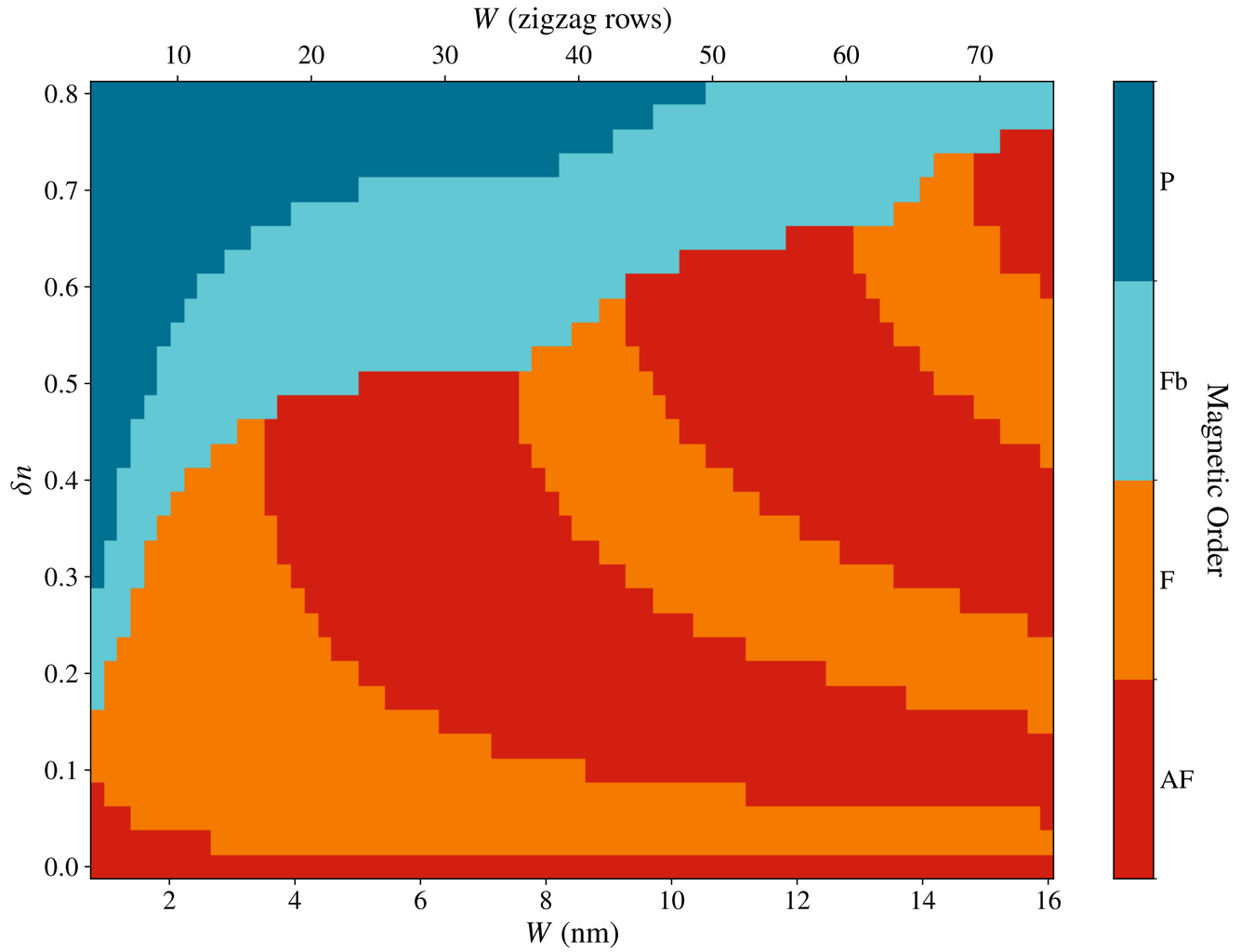

Correlation functions

- Two-point Green's function $C_{ij}(\tau)$

$$C_{ij}(\tau) = \langle c_i(\tau) c_j^\dagger(0) \rangle = \lim_{N_{\mathrm{cf}} \to \infty} \frac{1}{N_{\mathrm{cf}}} \sum_n M^{-1}[\{\phi\}_n]_{i\tau, j0}$$

- Interacting energies from the spectral decomposition

$$C_{ij}(\tau) = \frac{1}{Z} \sum_{m,n} \langle m | c_{i\tau} | n \rangle \langle n | c_{j0}^\dagger | m \rangle e^{-\beta E_m} e^{-\tau(E_n - E_m)}$$

$$\beta \to \infty \quad \to \sum_m \left(\langle 0 | c_{i\tau} | m \rangle \langle m | c_{j0}^\dagger | 0 \rangle e^{-(E_m - E_0)\tau} + \langle m | c_{i\tau} | 0 \rangle \langle 0 | c_{j0}^\dagger | m \rangle e^{-(E_m - E_0)(\beta - \tau)} \right)$$

Doping and chemical potential

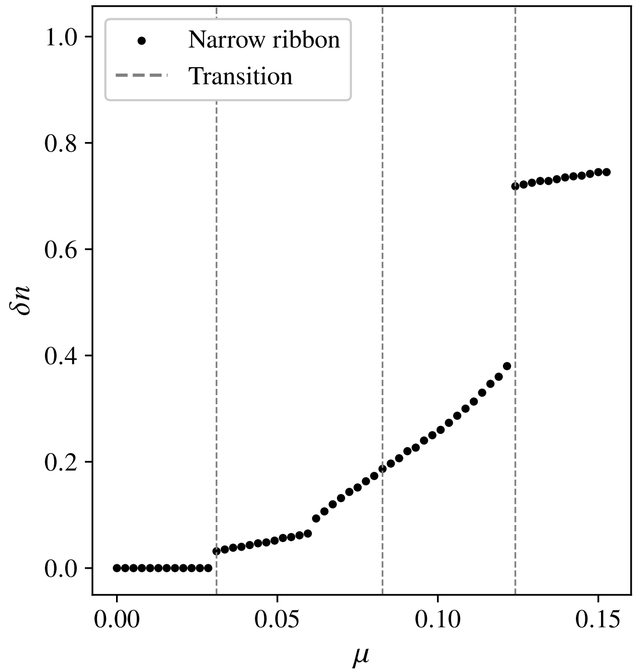

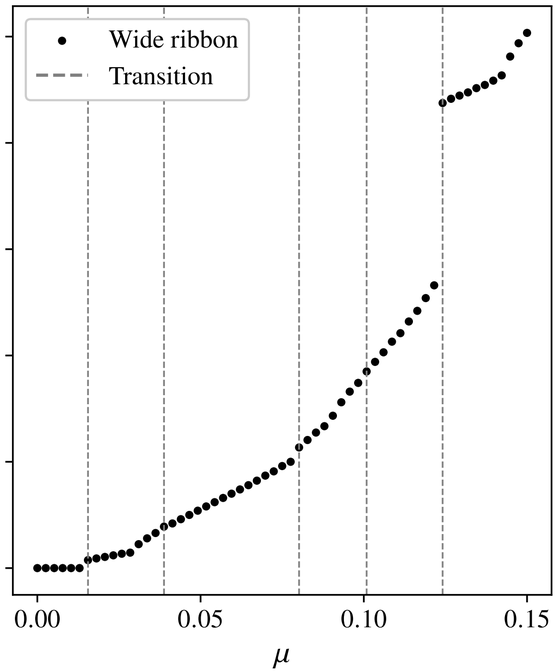

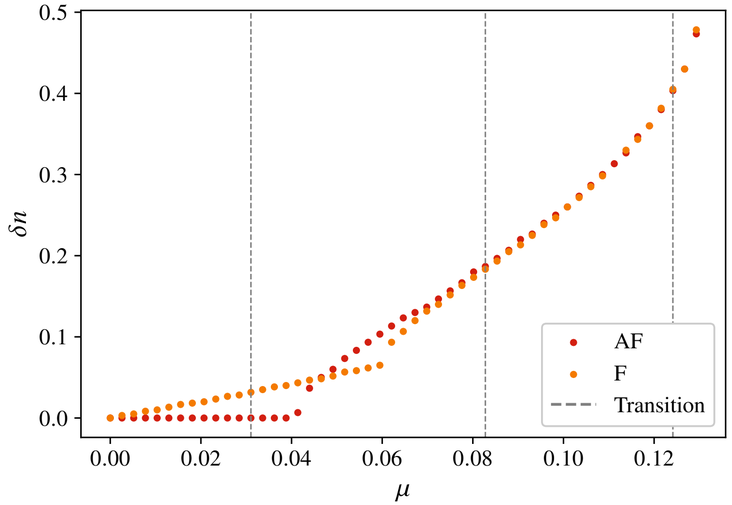

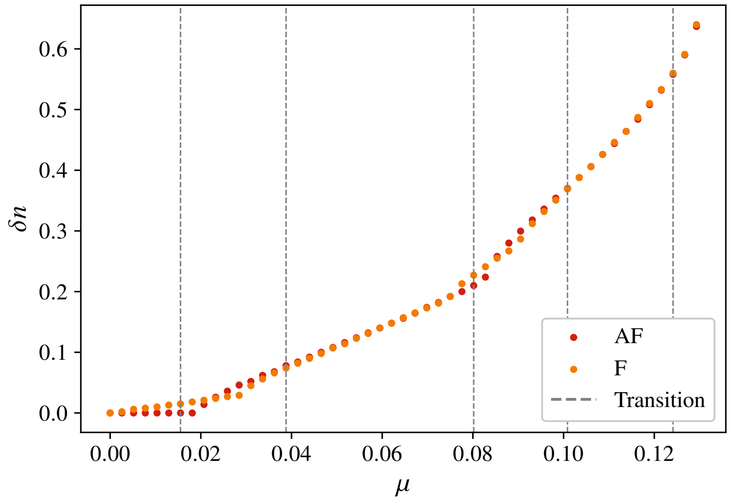

Non-zero chemical potential - Preliminary Results

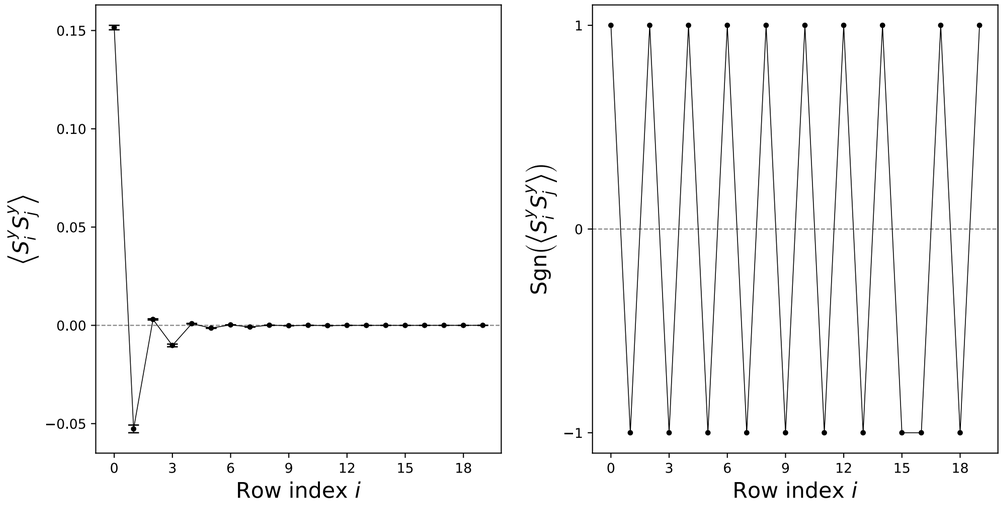

$\mu = 0.11$

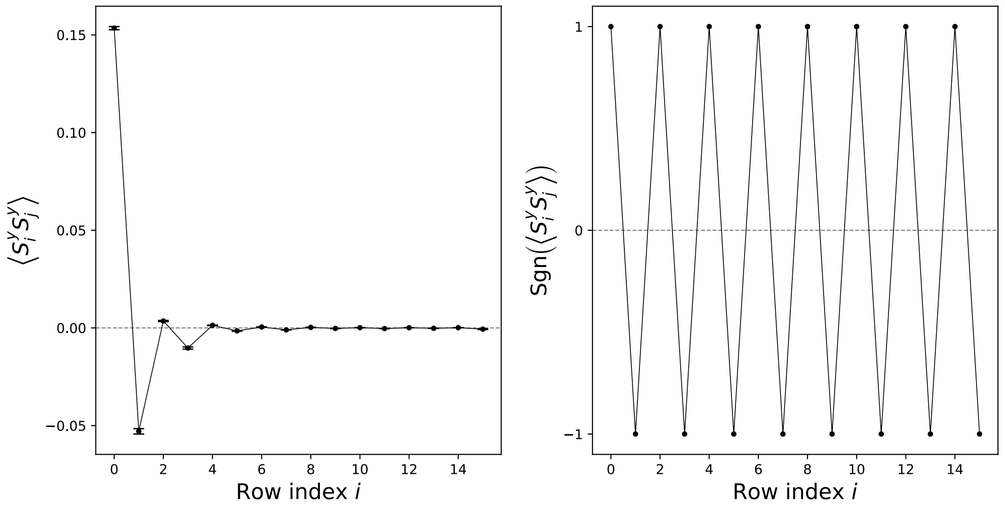

$\mu = 0.00$

$(N_x = 8, N_y = 8)$